Multiwavelength studies of the interstellar contents of gamma-ray bright supernova remnants

P. Dell'Ova, A. Gusdorf, M. Gerin

LERMA l'Observatoire de Paris ENS PSL Université Paris

INTRODUCTION

How to interpret gamma-ray observations ?
The supernova remnant IC443

REVIEW : CHARACTERIZING THE INTERSTELLAR MEDIUM OF SUPERNOVA REMNANTS

Atomic and molecular lines,

Dust thermal emission,

Magnetic field,

Star formation,

SUMMARY AND OUTLOOK


cta
cherenkov telescope array

Multi-phase medium :

- gas, grains (~1 % of the mass)
- various ionization states
- various densities (~10^{-3} to 10^{6} cm^{-3})
- various temperatures (~10 to 10^{6} K)

Multi-scales (coupled) :

- Molecular clouds, SNR cavities (~10 pc)
- Protostars (~10 au)

Various radiation fields :

- from radio waves to gamma rays
- magnetic fields

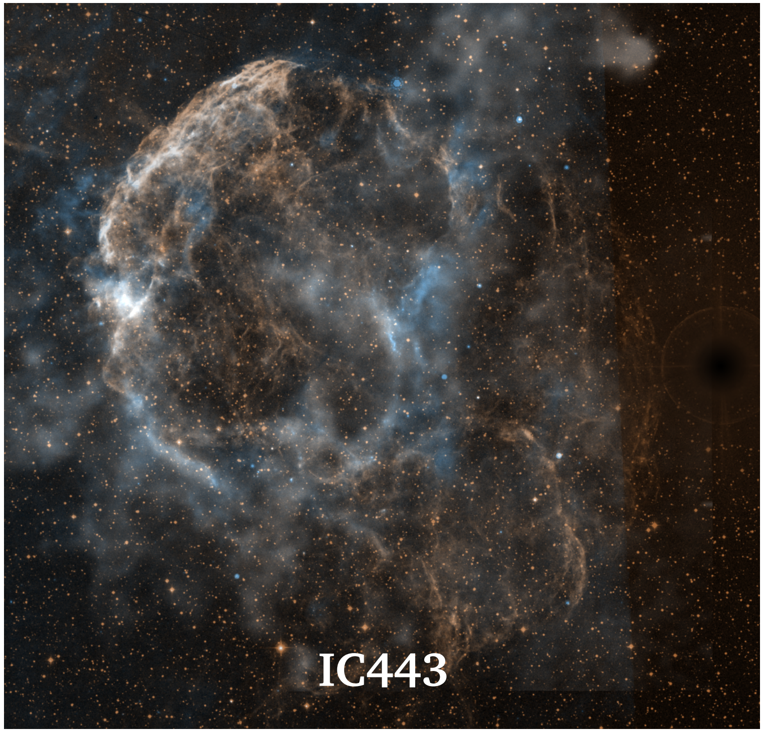

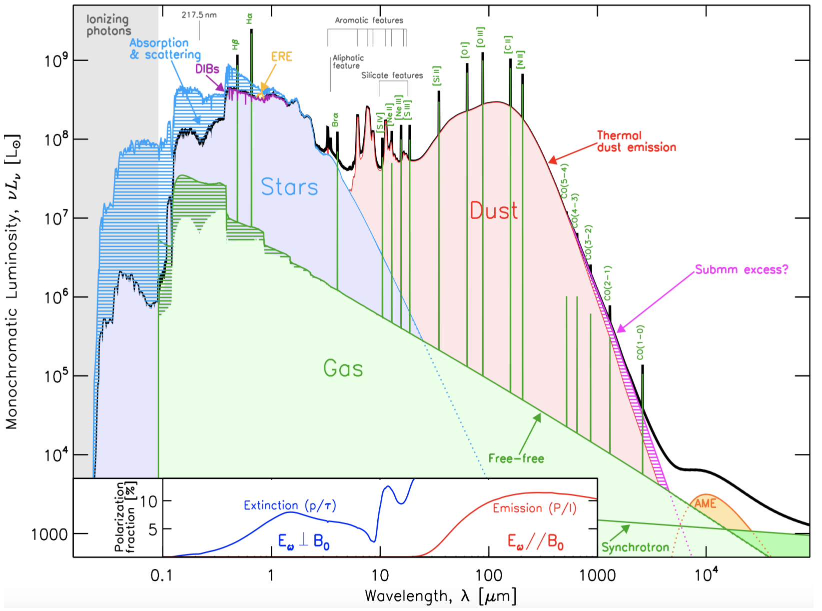

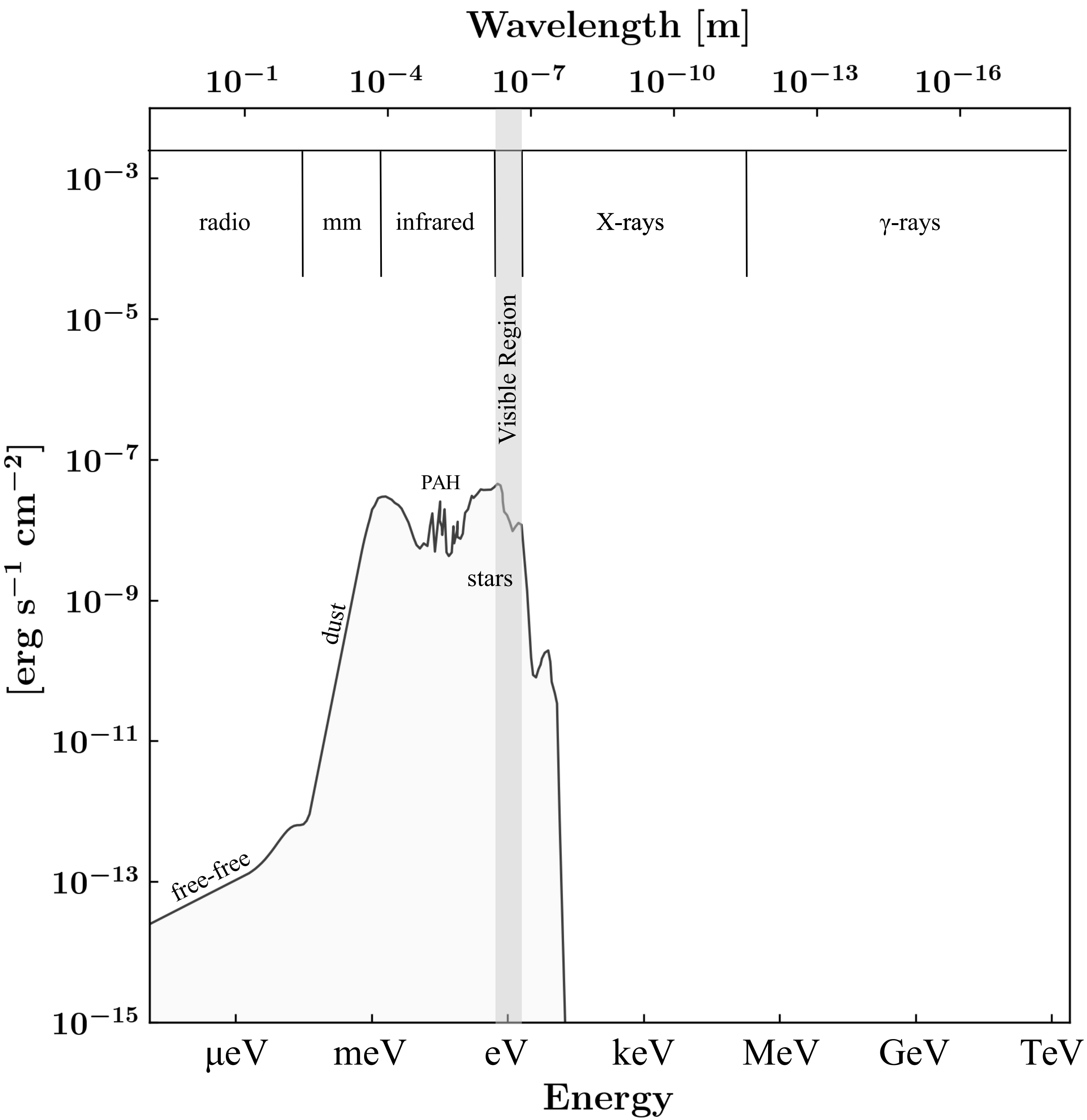
Wavelength [m]
10^{-1}
10^{-4}
10^{-7}
10^{-10}
10^{-13}
10^{-16}
radio
mm
infrared
X-rays
γ-rays
Visible Region
PAH
stars
dust
free-free
[erg s^{-1} cm^{-2}]
10^{-3}
10^{-5}
10^{-7}
10^{-9}
10^{-11}
10^{-13}
10^{-15}
μeV
meV
eV
keV
MeV
GeV
TeV
Energy

ISM + **leptonic** cosmic-rays

Synchrotron

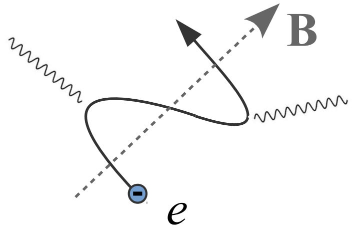

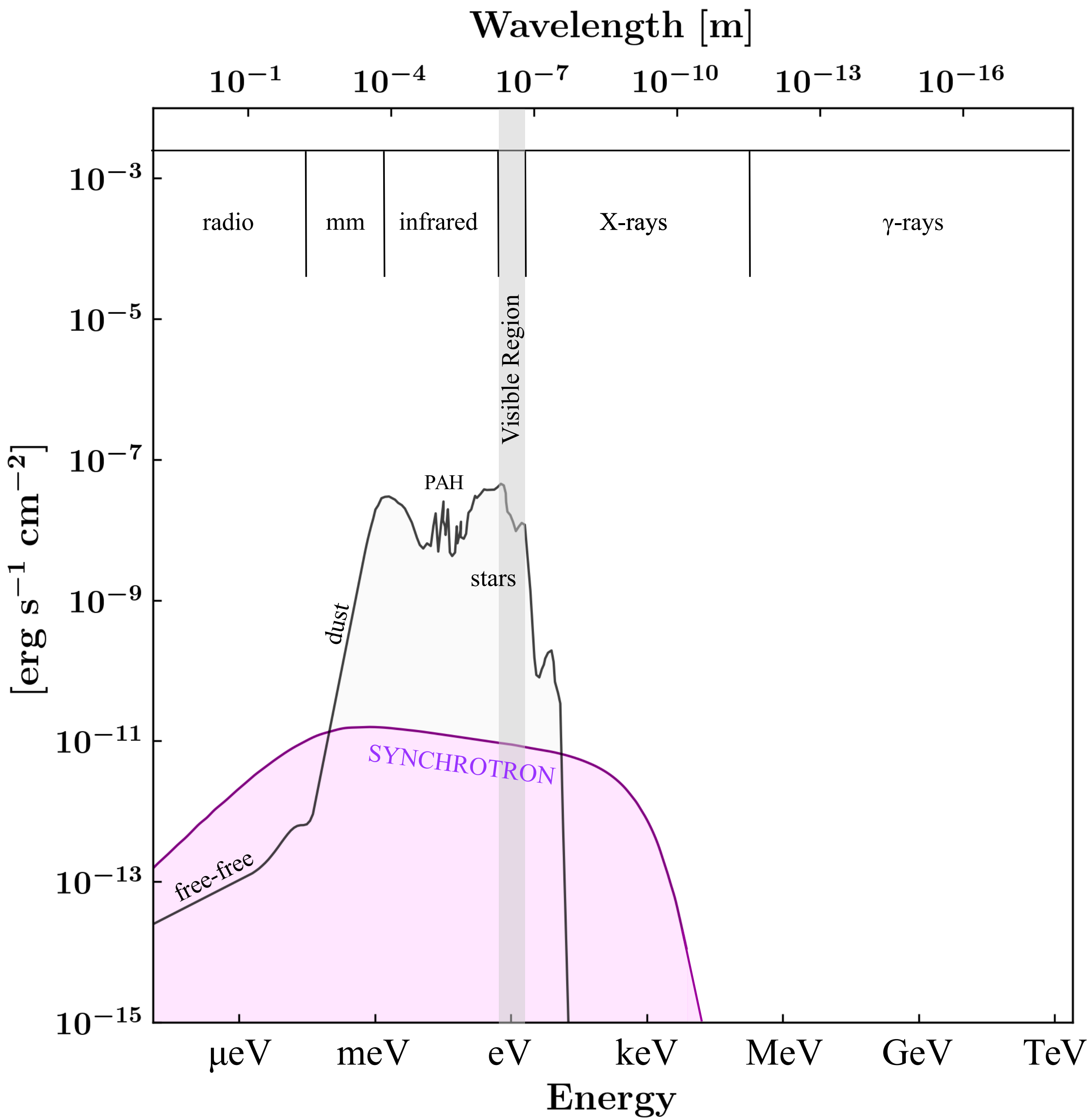

ISM + **leptonic** cosmic-rays

Synchrotron

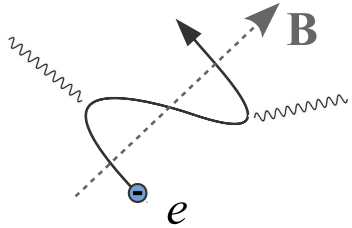

Inverse Compton scattering

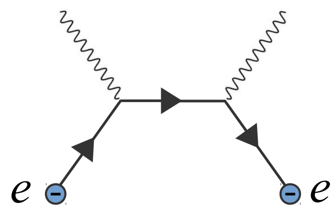

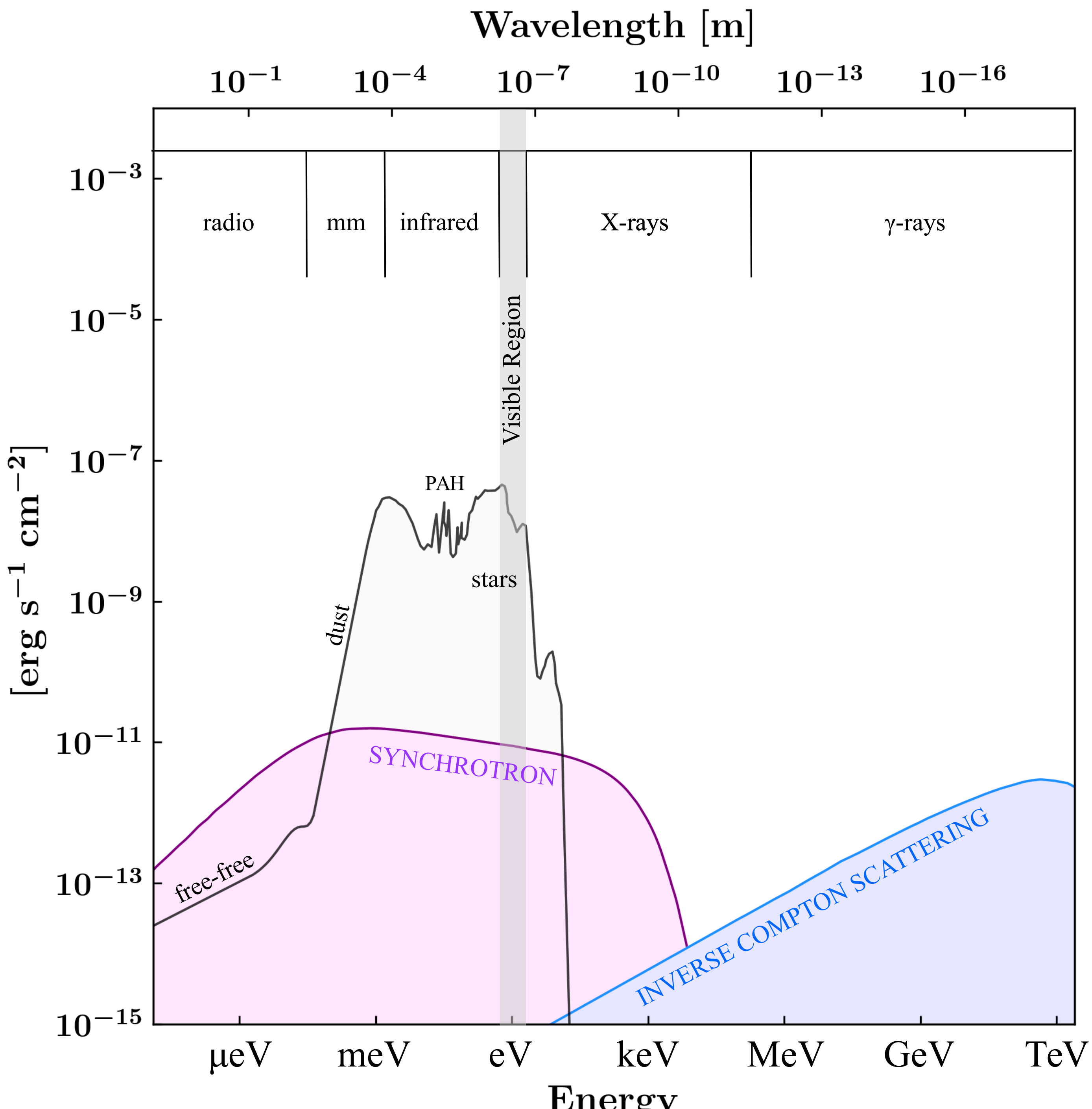

ISM + **leptonic** cosmic-rays

Synchrotron

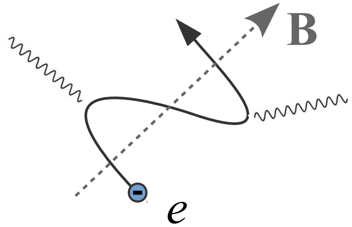

Inverse Compton scattering

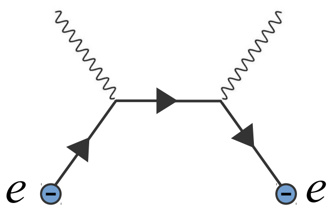

Bremsstrahlung

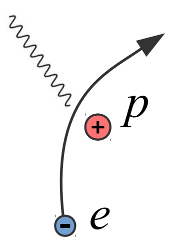

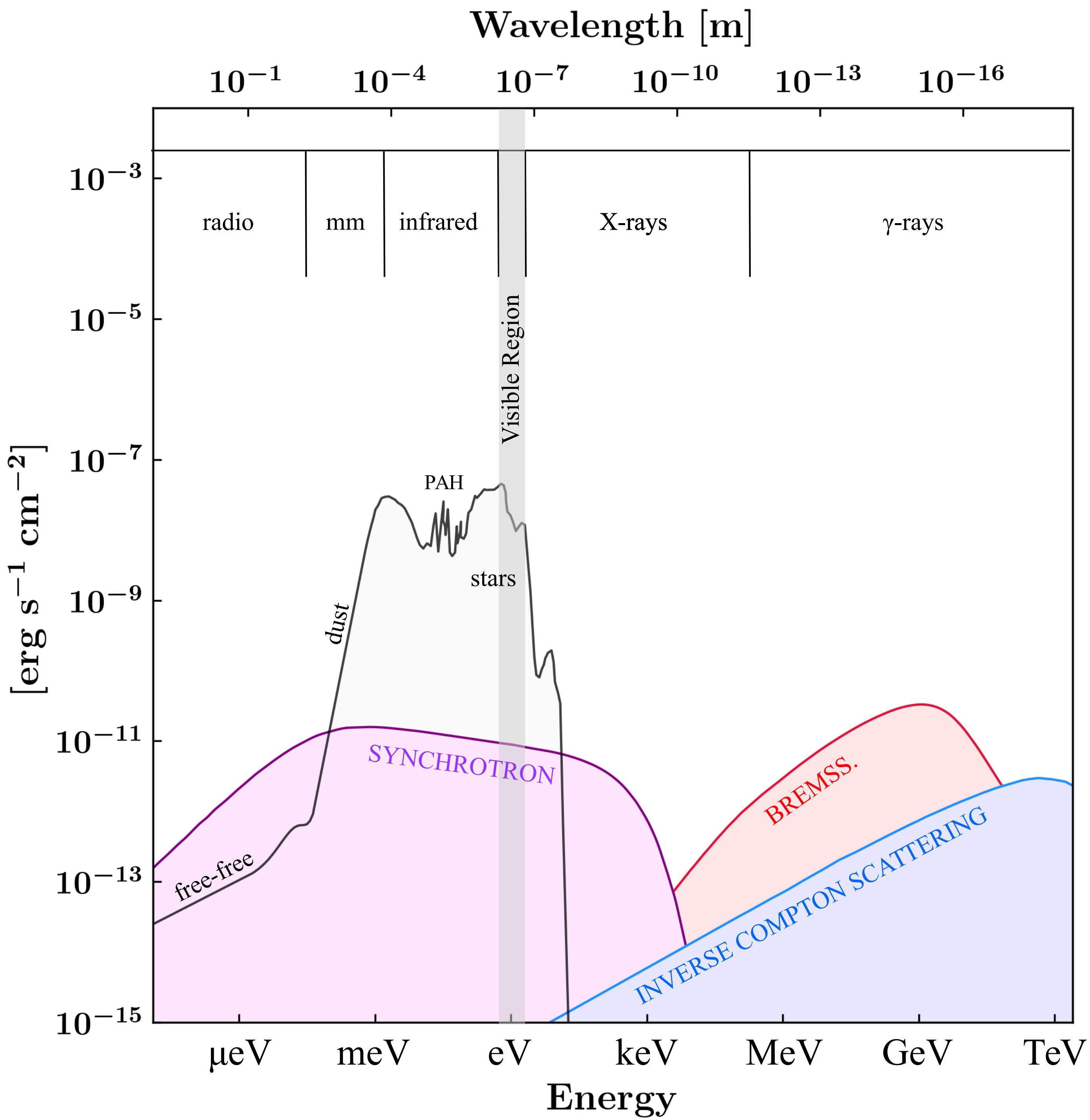

ISM + **leptonic** cosmic-rays

Synchrotron

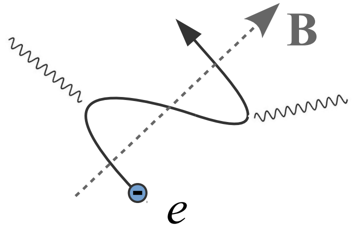

Inverse Compton scattering

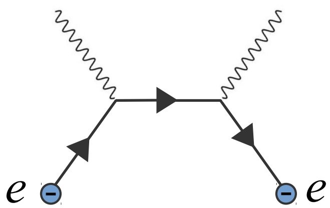

Bremsstrahlung

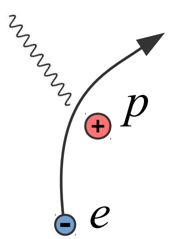

ISM + **hadronic** cosmic-rays

Pion decay

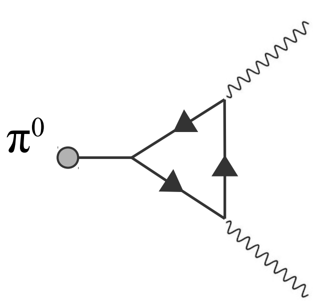

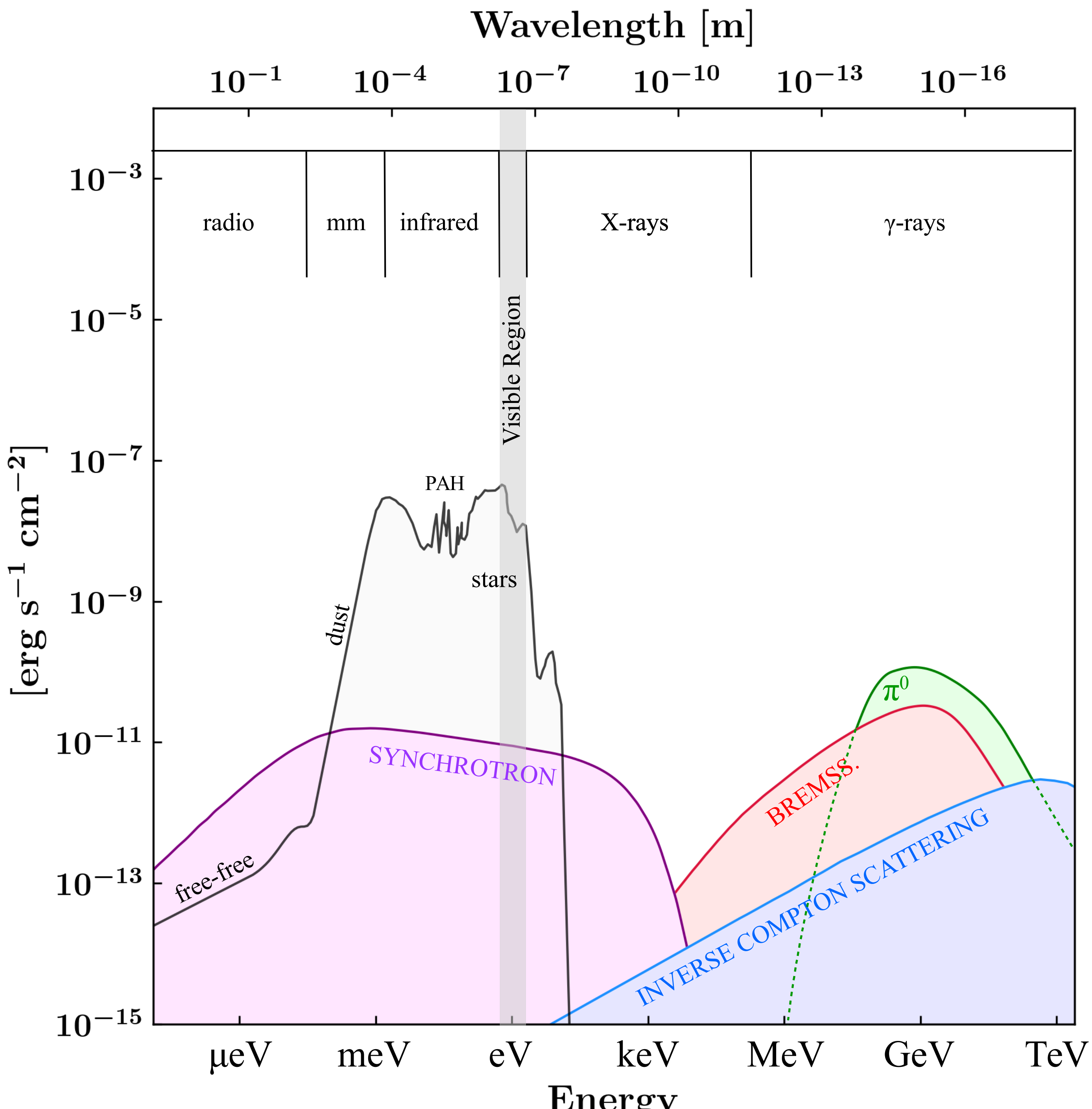

ISM + **leptonic** cosmic-rays

Synchrotron

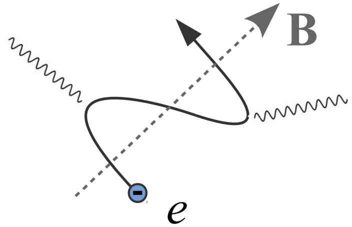

Inverse Compton scattering

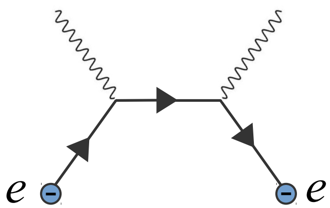

Bremsstrahlung

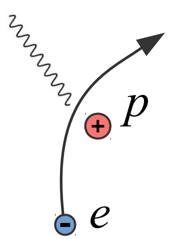

ISM + **hadronic** cosmic-rays

Pion decay

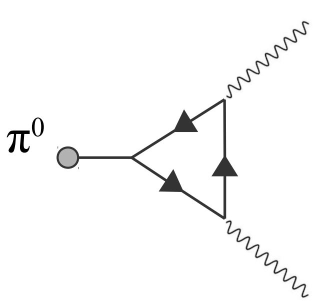

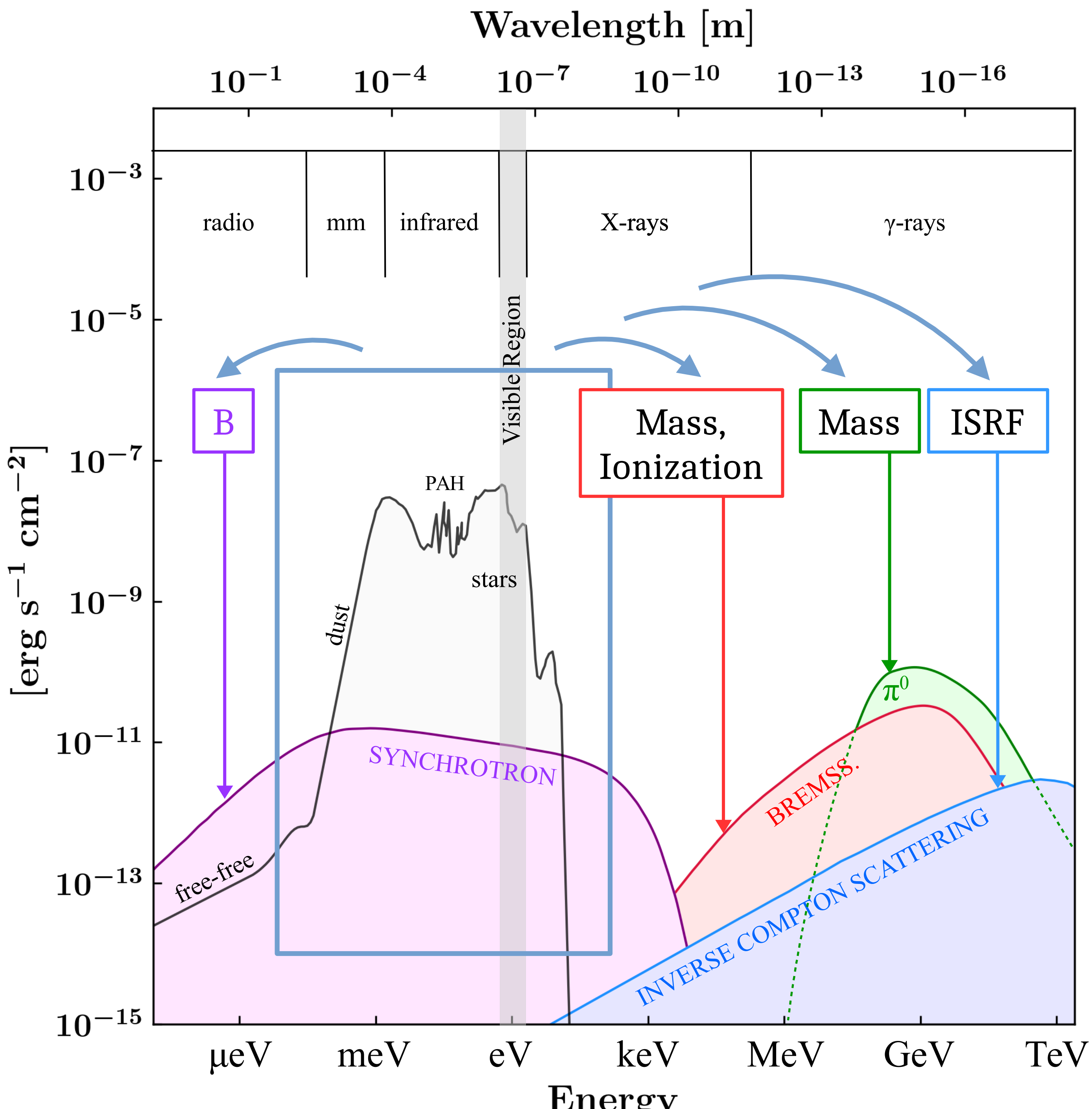

Galliano *et al.* 2018

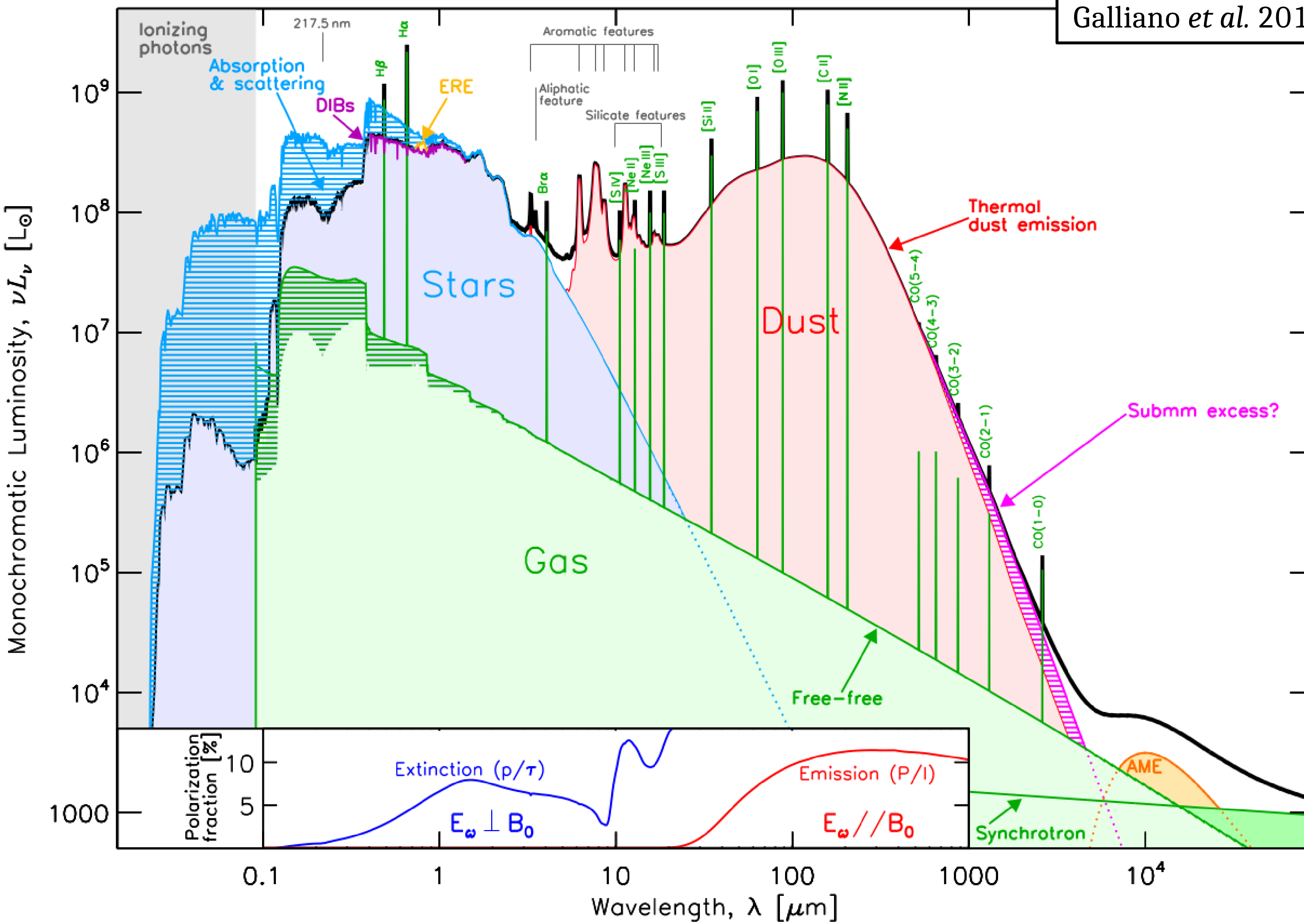

The supernova remnant IC443

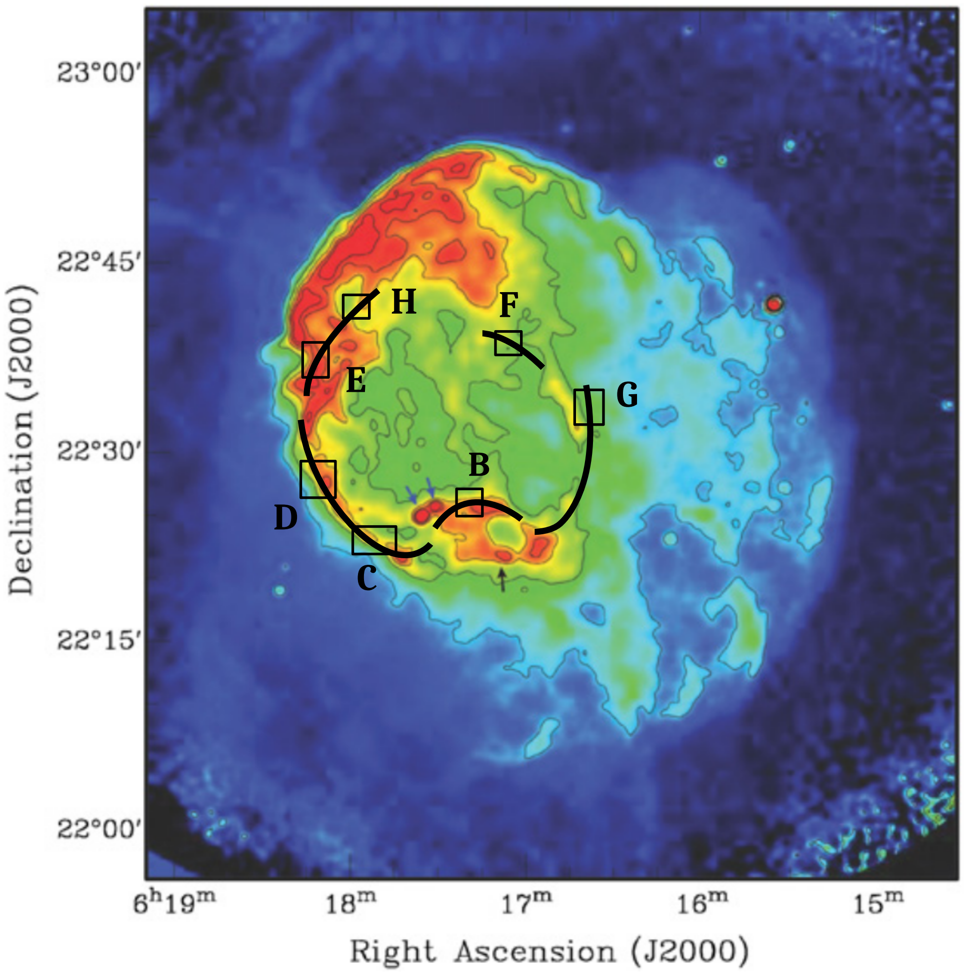

21cm radio continuum

Lee *et al.* (2008)

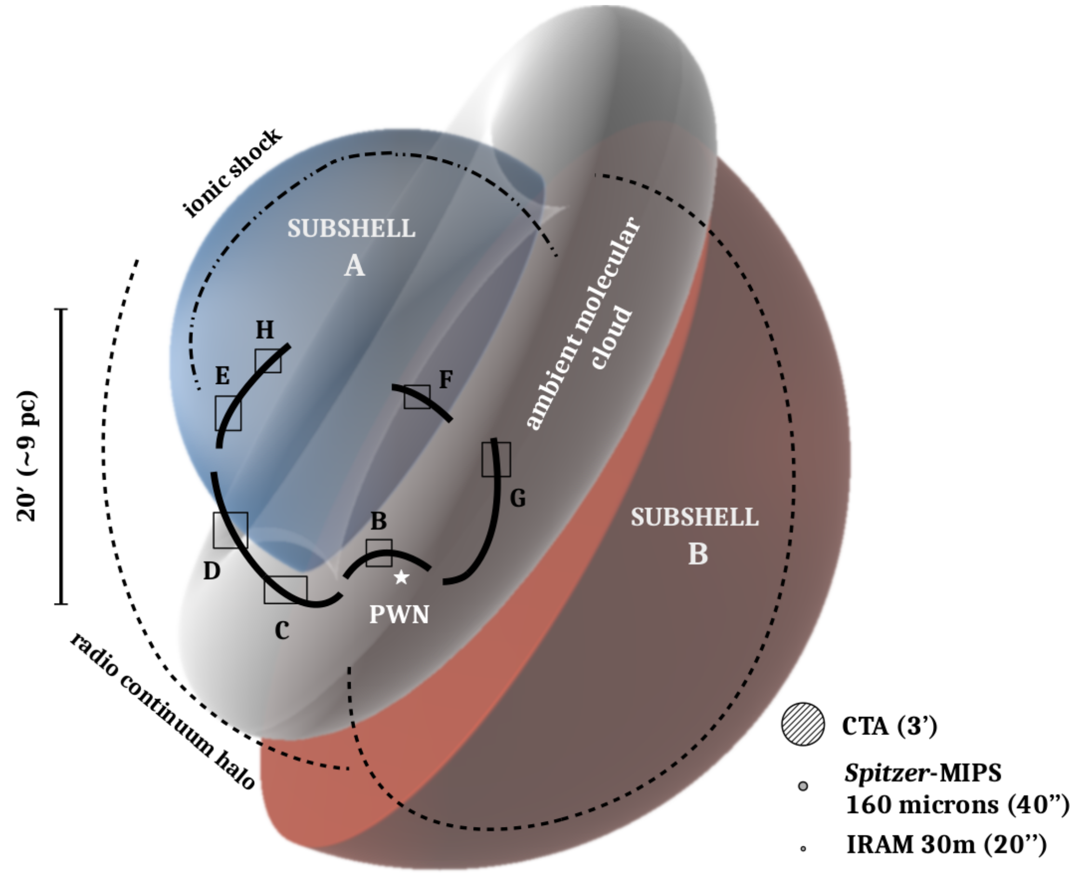

multiwavelength

Lee *et al.* (2008, 2012)
Troja *et al.* (2008)
Dickman *et al.* (1992)

VHE emission models of IC443 are partially degenerate.

Can we better constrain the interstellar contents ?

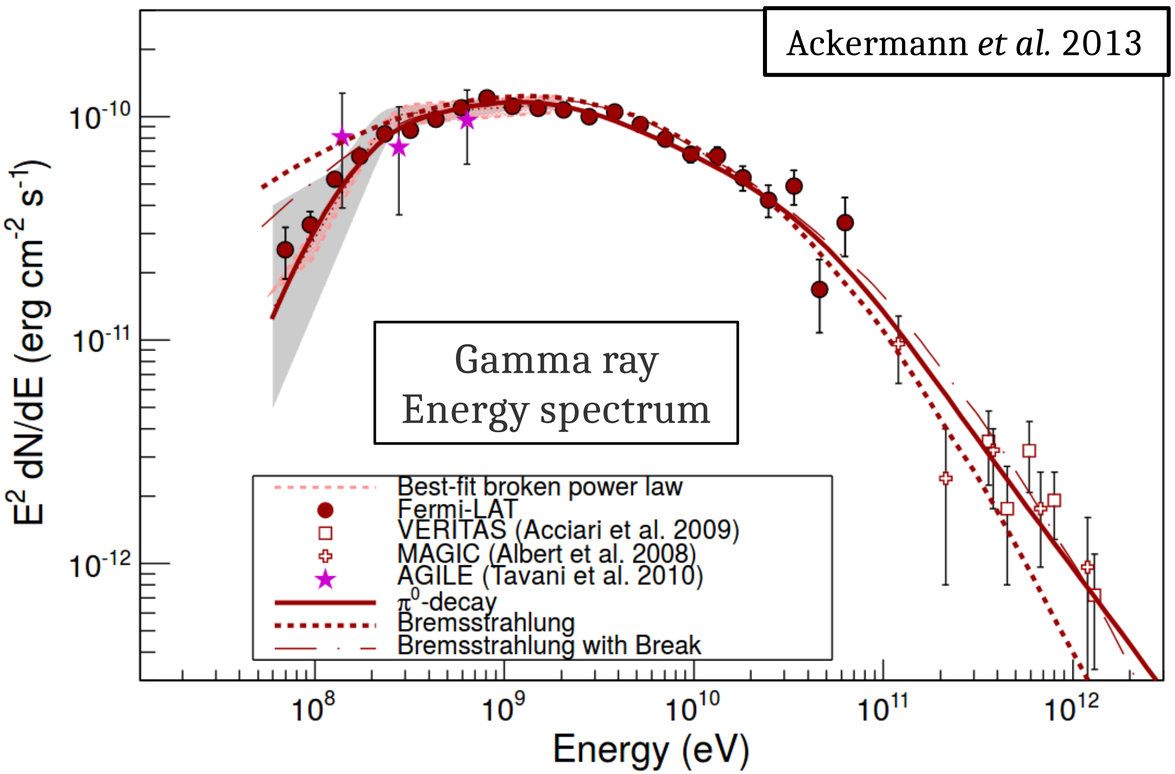

Atomic and molecular phases

HI, ^{12}CO and H_2 observations

Arecibo,
WSRT,
GMRT,
FAST

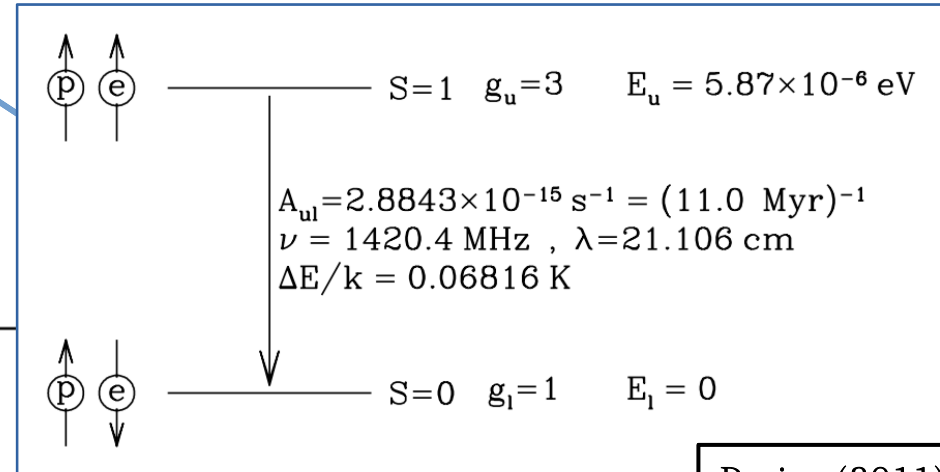

Draine (2011)

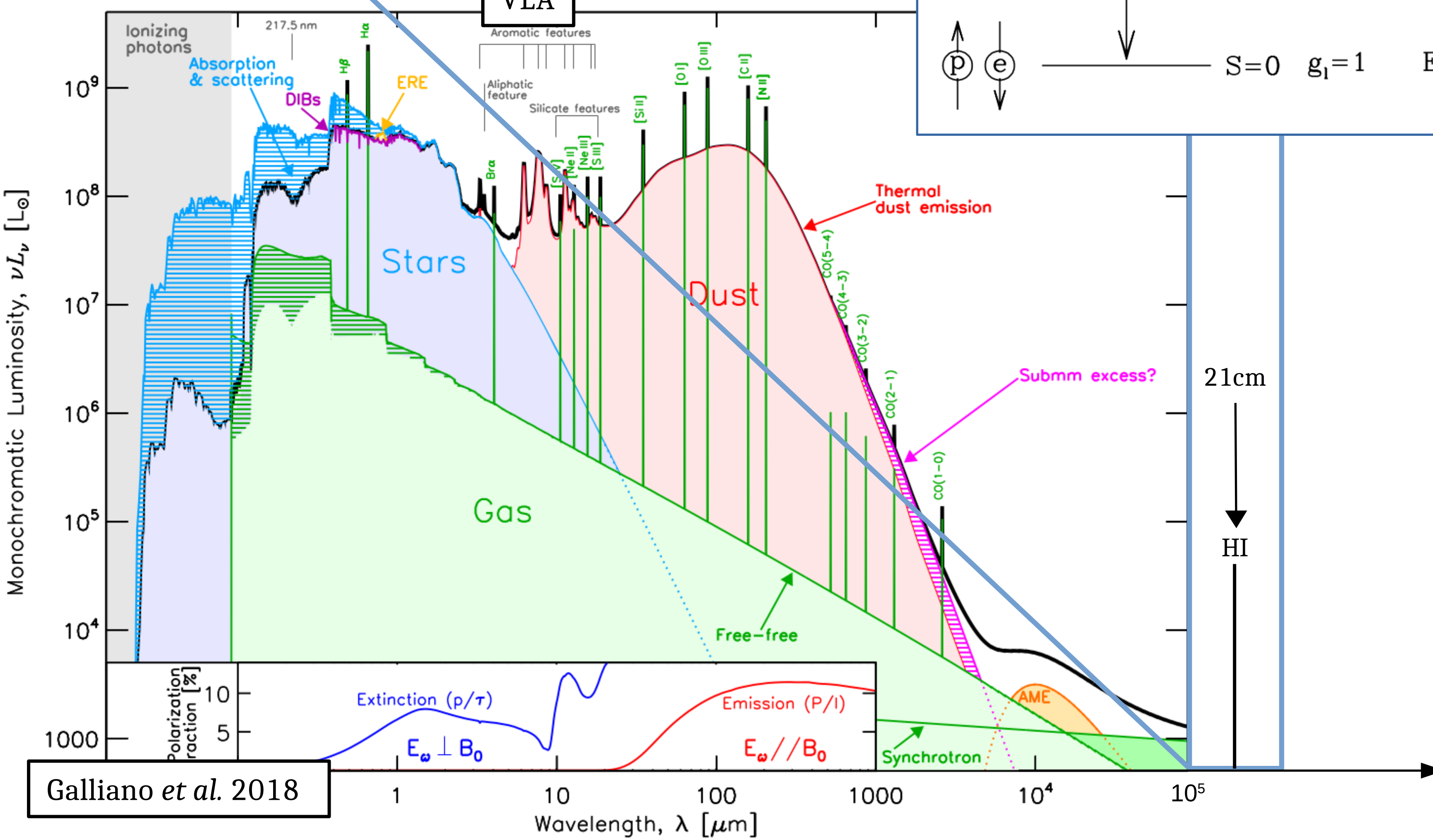

Galliano *et al.* 2018

Lee *et al.* 2008

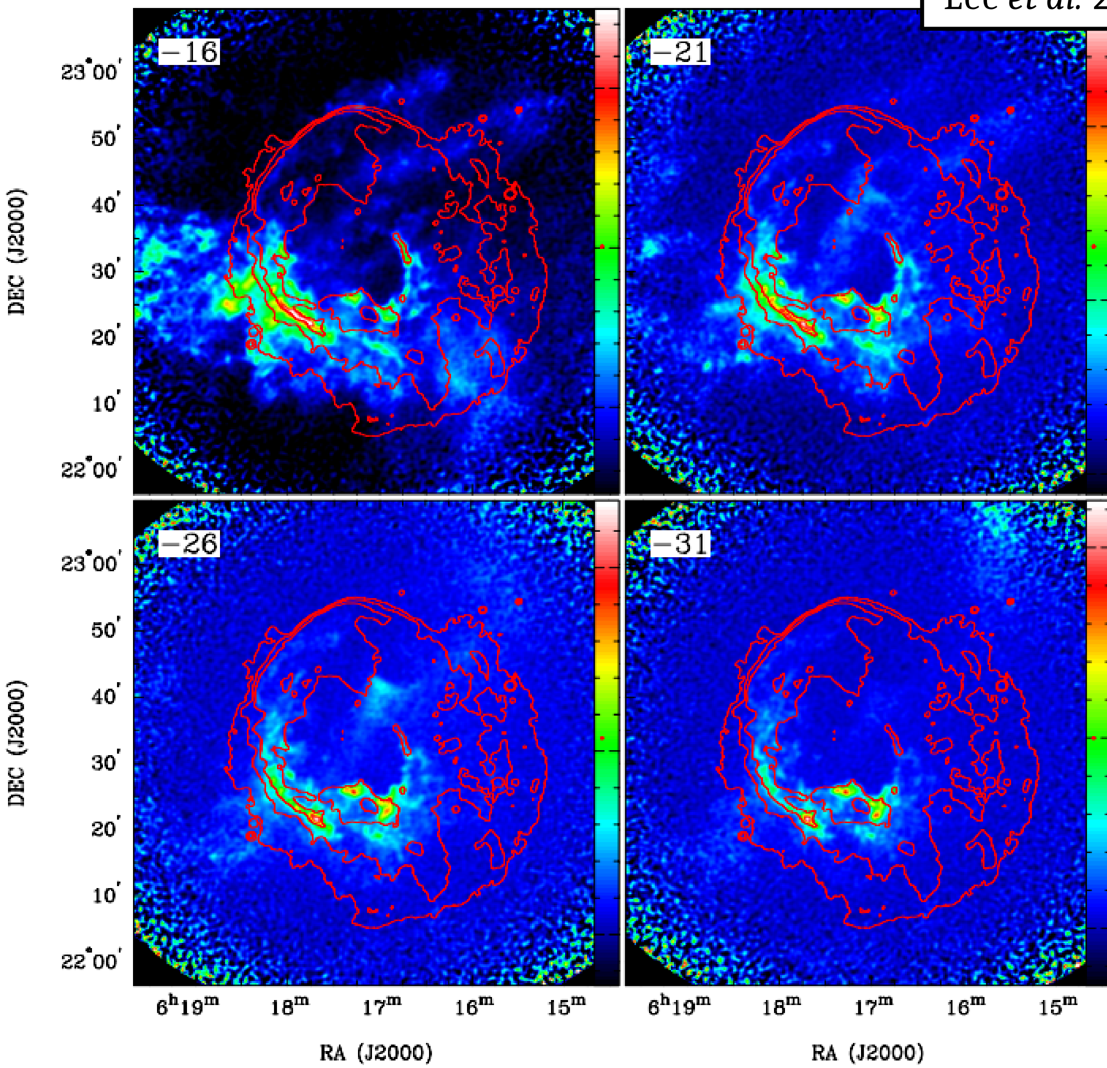

Lee *et al.* 2008

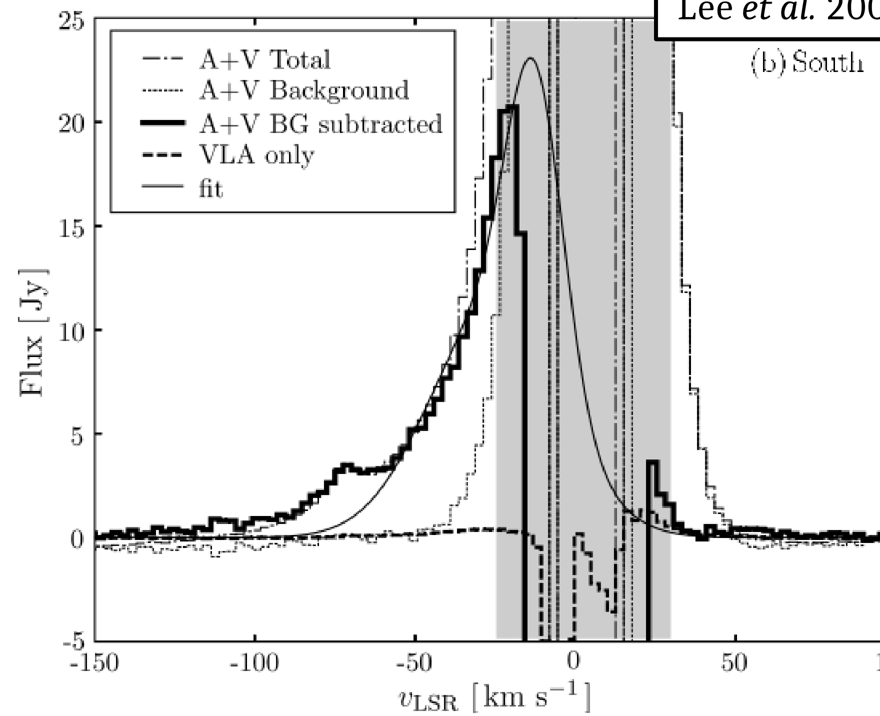

$$M_{\rm H\,I} = \frac{16\pi m_{\rm H}}{3A_{ul}hc} D_L^2 \int F_\nu dv$$

MOLECULAR PHASE : Observations of CO lines

^{12}CO, ^{13}CO, $C^{18}O$
Rotational transitions
J=1-0, J=2-1, J=3-2

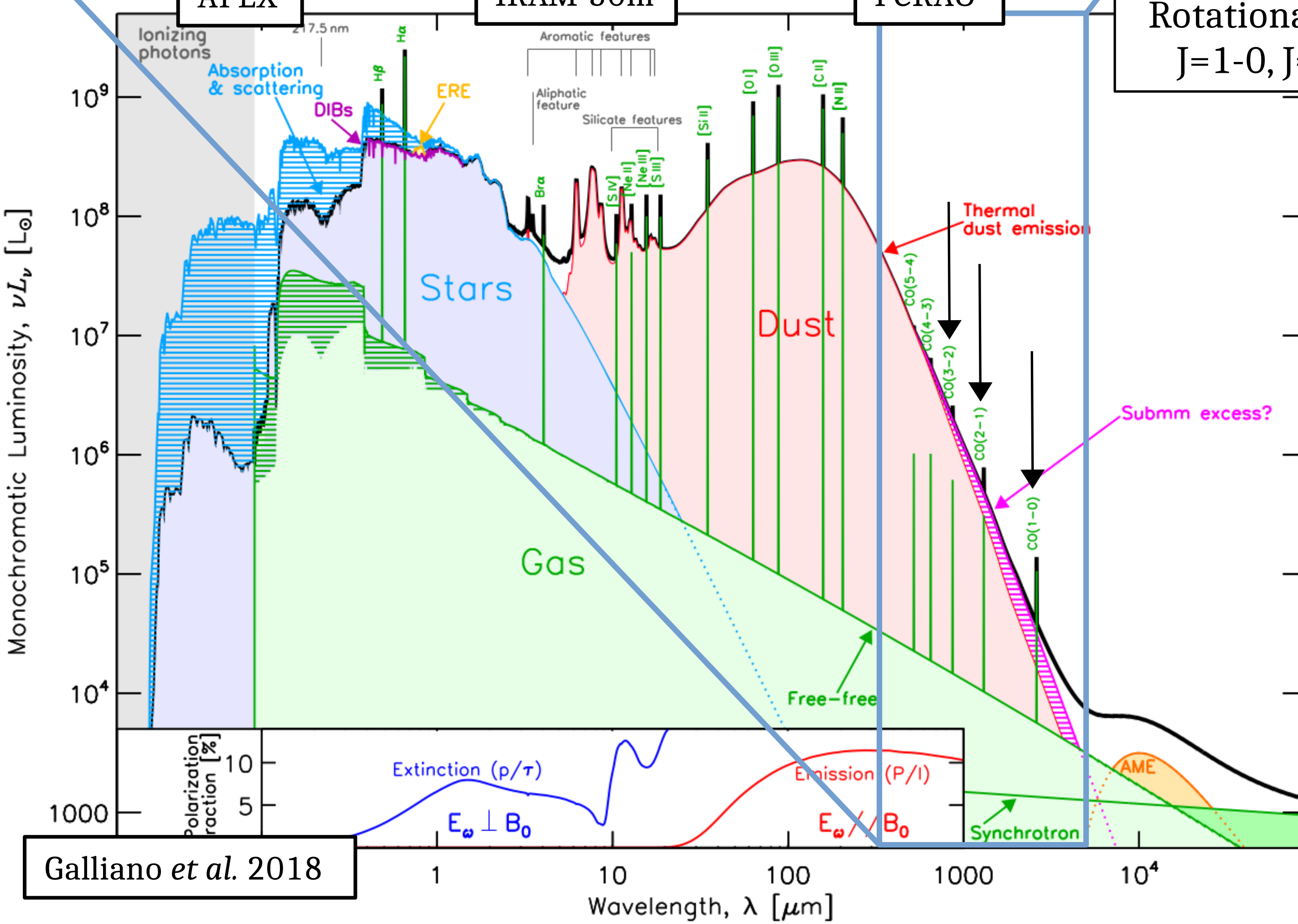

Galliano *et al.* 2018

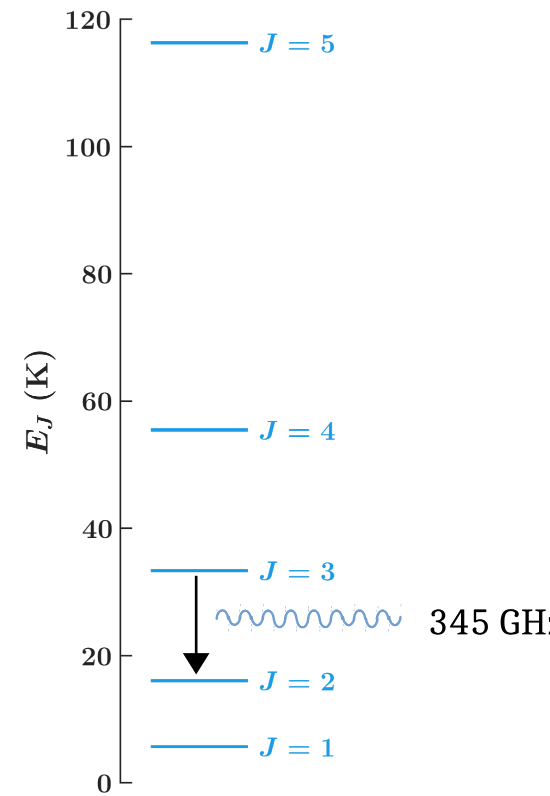

Brightness temperature maps

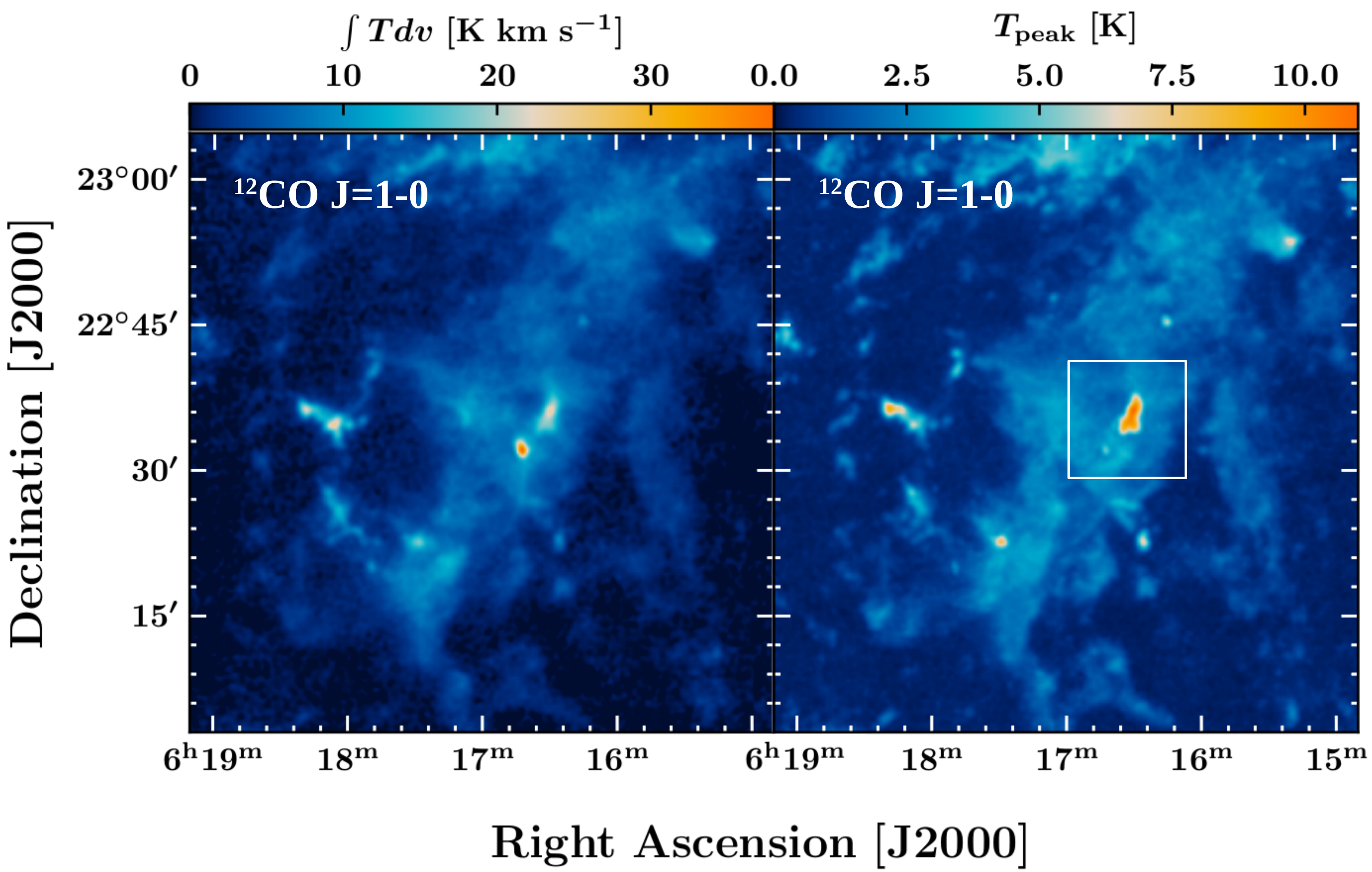

FCRAO

Lee *et al.* 2012

Brightness temperature maps

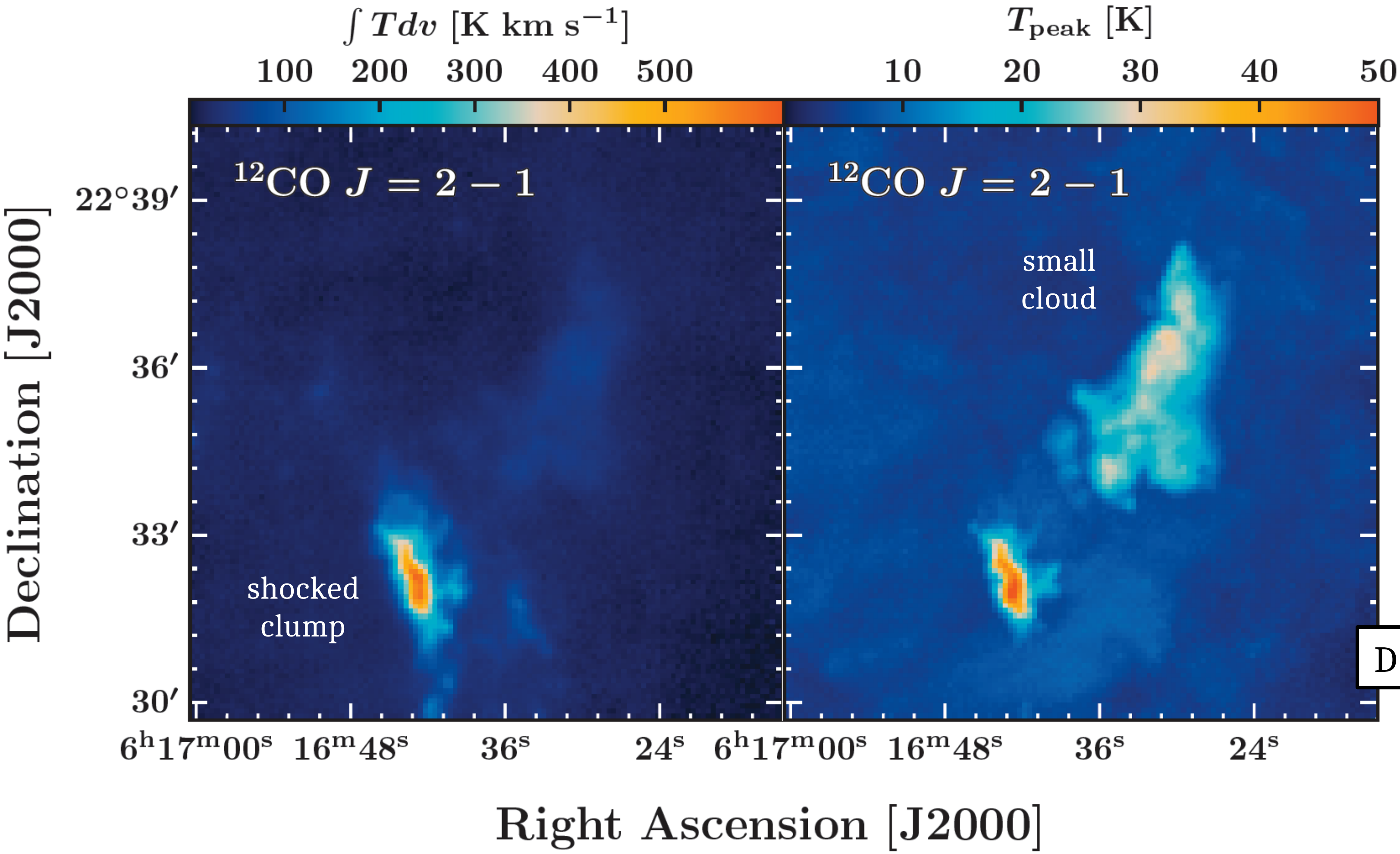

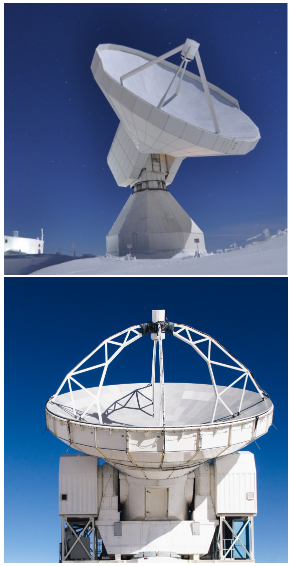

Dell'Ova *et al.* 2020

MOLECULAR PHASE : Observations of CO lines

^{12}CO spectra

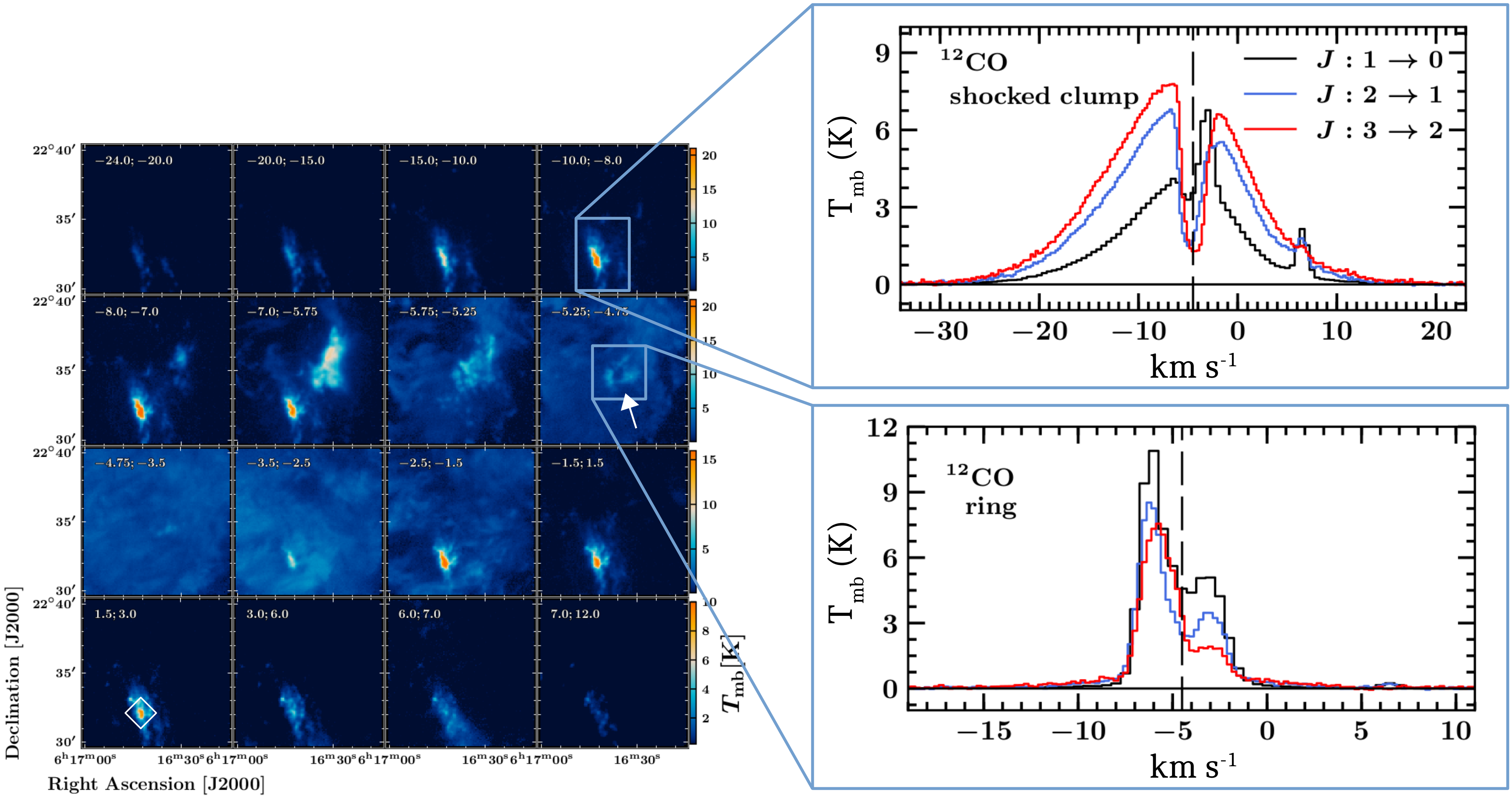

- $\sum I_\nu \cdot \Delta\nu$ is in erg/s/cm^2/sr

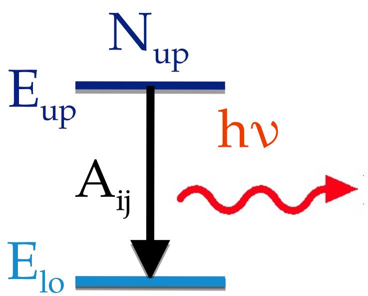

- $\sum I_\nu \cdot \Delta\nu = \frac{1}{4\pi} h\,\nu_{ij} A_{ij} N_{up}$
- $\frac{2\,k_B\,\nu_{ij}^3}{c^3} \sum T_{mb} \cdot \Delta v = \frac{1}{4\pi} h\,\nu_{ij} A_{ij} N_{up}$
    - Solid angle normalization (sr^{-1})
    - Energy of one photon from the transition (erg)
    - Probability of the transition (s^{-1})
    - Column density of the molecules in the upper state (cm^{-2})

- Relation between N_i and N_{tot} : $\frac{N_i}{g_i} = N_{tot} \cdot \frac{exp\,(-\frac{E_i}{k_B\,T_{ex}})}{Q(T_{ex})}$

- Excitation diagram represents $\{ln(\frac{N_i}{g_i})\}$ vs. $\{\frac{E_i}{k_B}\}$:

$$ln\,(\frac{N_i}{g_i}) = [ln\,(N_{tot}) - ln\,(Q(T_{ex}))] - \frac{E_i}{k_B\,T_{ex}}$$

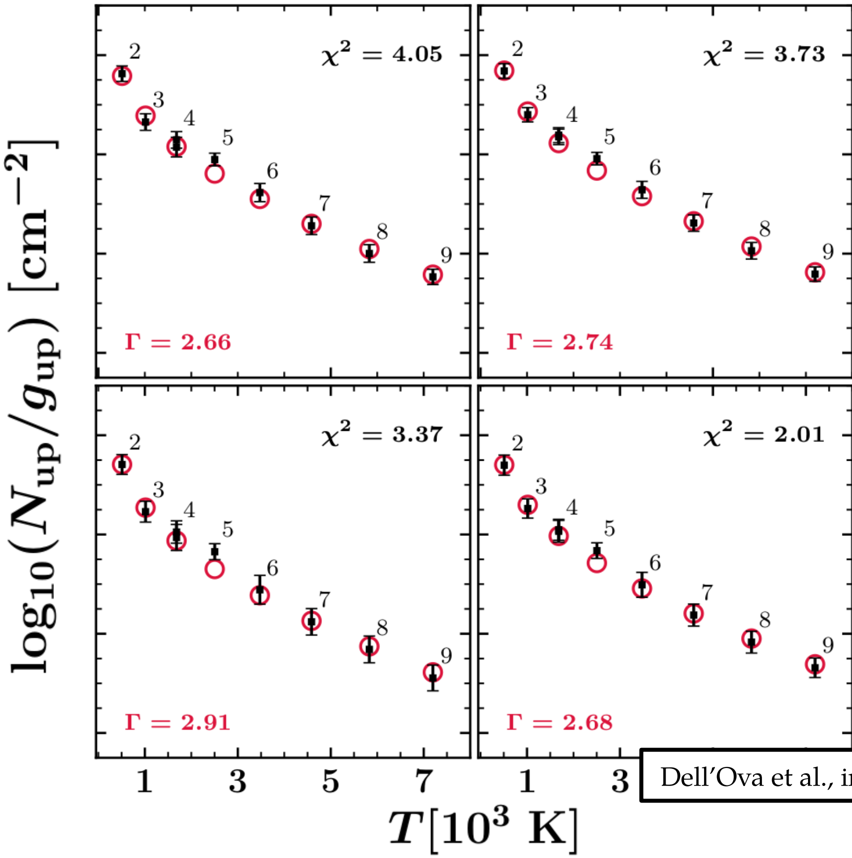

Dell'Ova et al., in prep

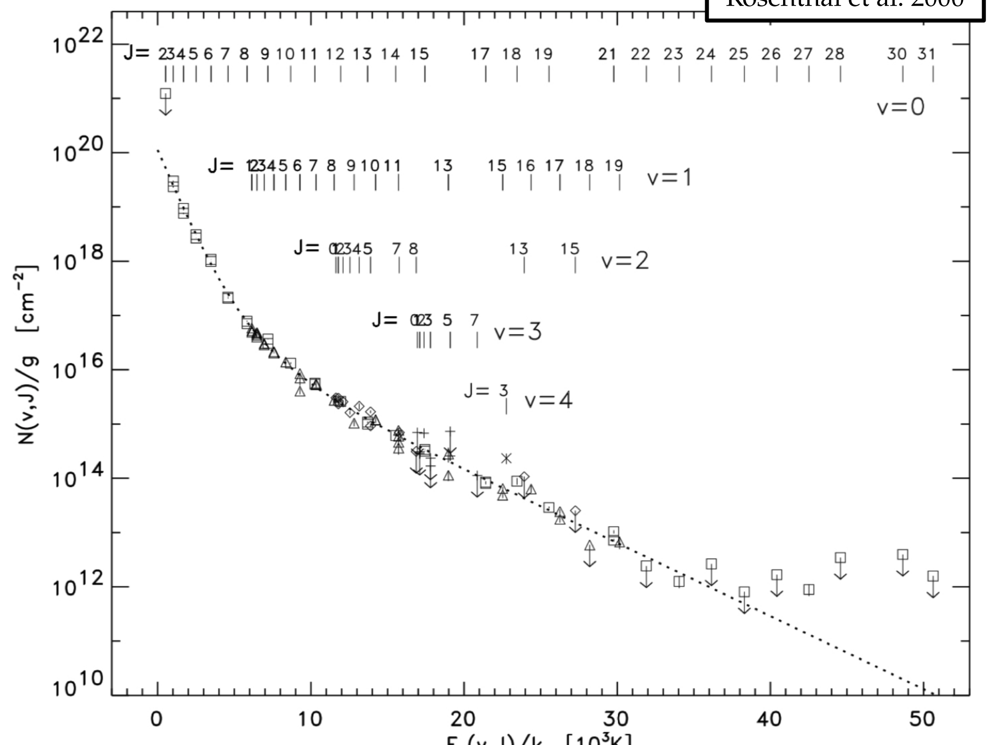

Rosenthal et al. 2000

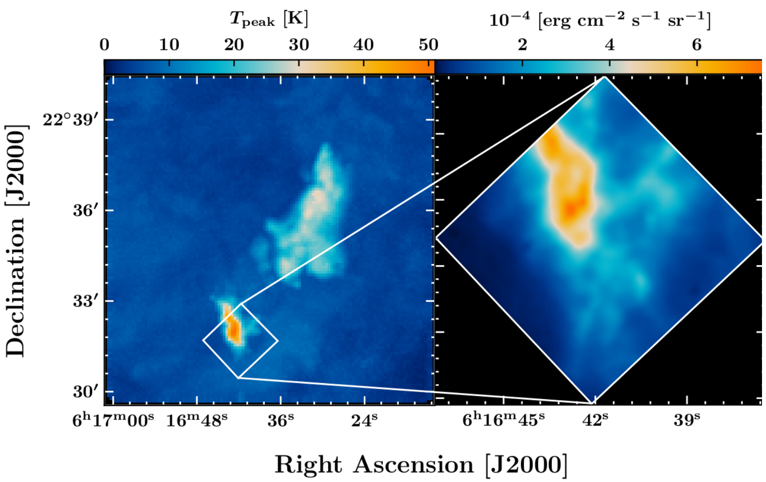

H_2 temperature tomography

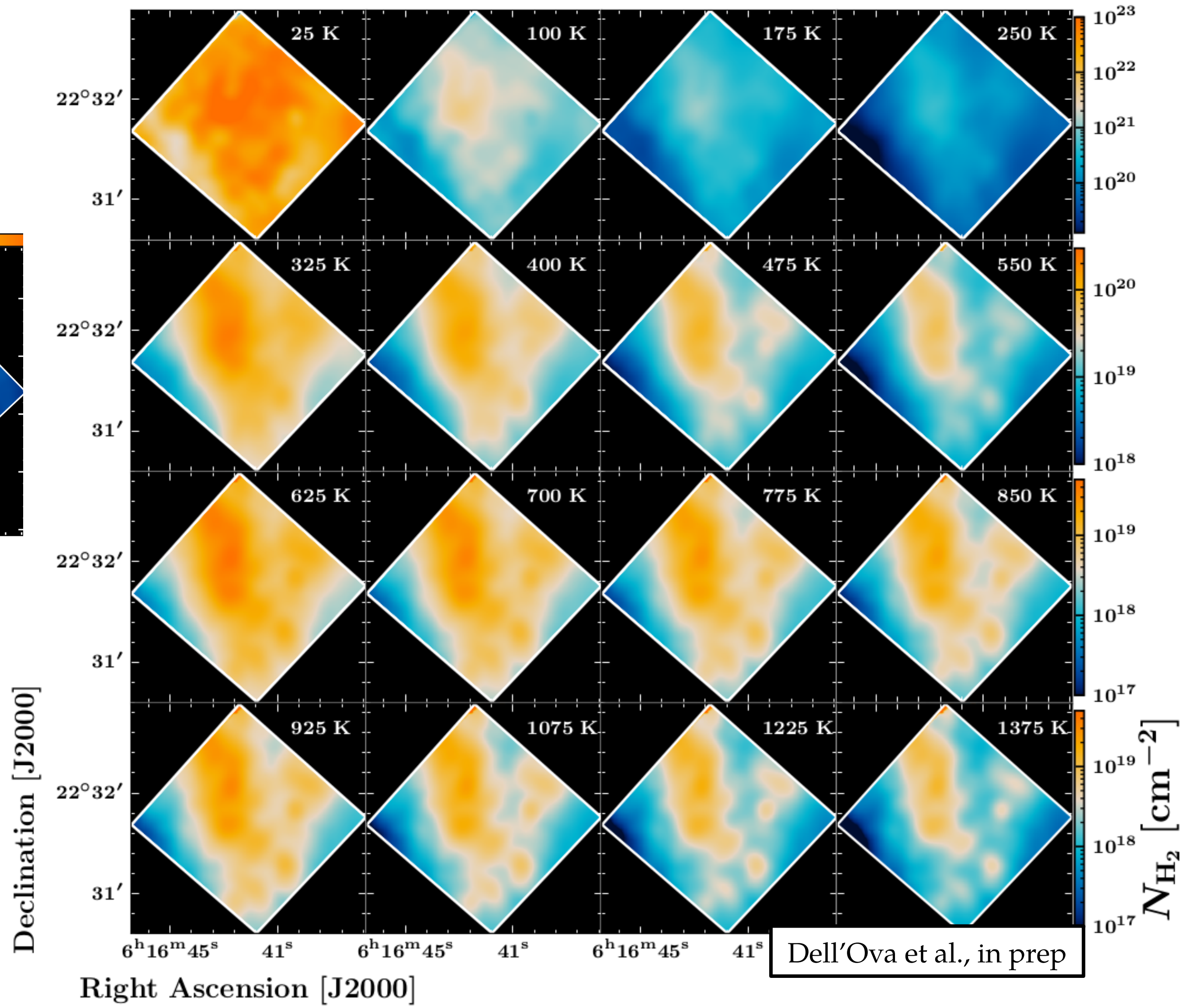

Dell'Ova et al., in prep

Van der Tak *et al.* 2007

Second method : use RADEX.

(statistical equilibrium radiative transfer with the Large Velocity Gradient approximation)

$$\frac{dn_i}{dt} = \sum_{i \neq j} n_j \Gamma_{ji} - n_i \sum_{i \neq j} \Gamma_{ij}$$

$$\Gamma_{ij} = \begin{cases} A_{ij} + B_{ij}\overline{J_\nu} + C_{ij} & (i > j) \\ B_{ij}\overline{J_\nu} + C_{ij} & (i < j) \end{cases}$$

RADEX solves this, assuming :

(1) $\overline{J_\nu} = S_\nu(1 - \beta)$ (2) $\beta = \frac{1 - e^{-\tau}}{\tau}$

Chi-square minimization (small cloud)

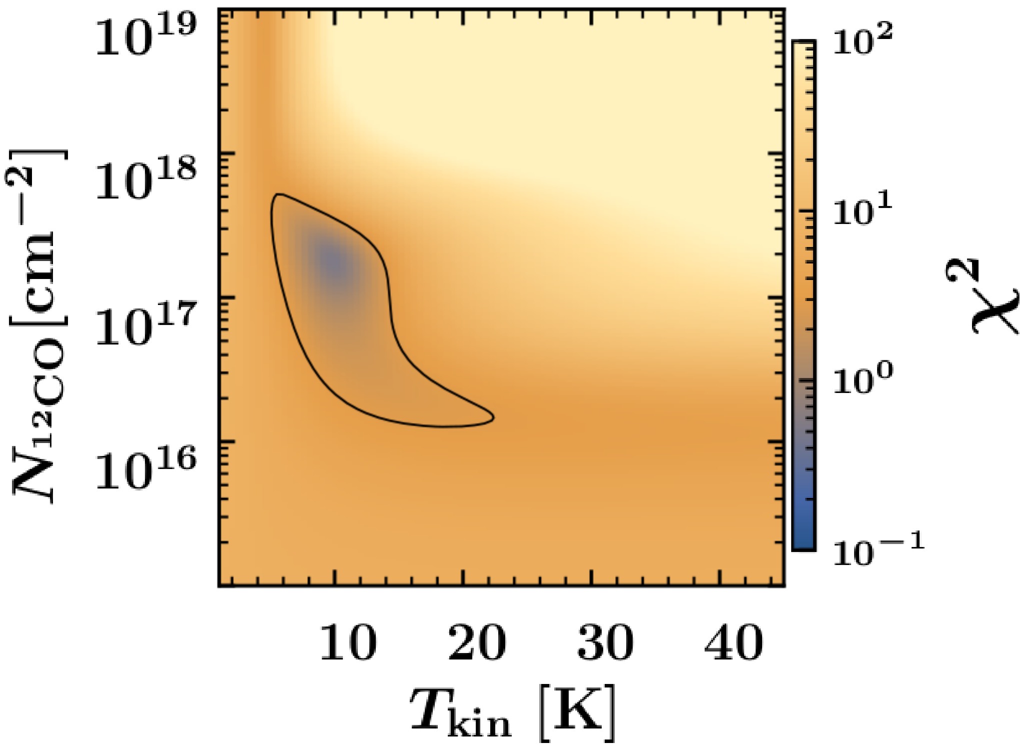

Compare observations with a grid of RADEX models

Dell'Ova *et al.* 2020

The Paris-Durham molecular shock model

Developed continuously since 30 yrs *Flower, D. R., Pineau des Forets, G., & Hartquist, T. W. , 1985, MNRAS, 216, 775* ***+ 40 papers thereafter***

- multi-fluid MHD shock (C, J, C+J)
- Steady, plane-parallel (1D)
- Chemistry: 136 species (in gas, ices, grain cores), about 1000 reactions

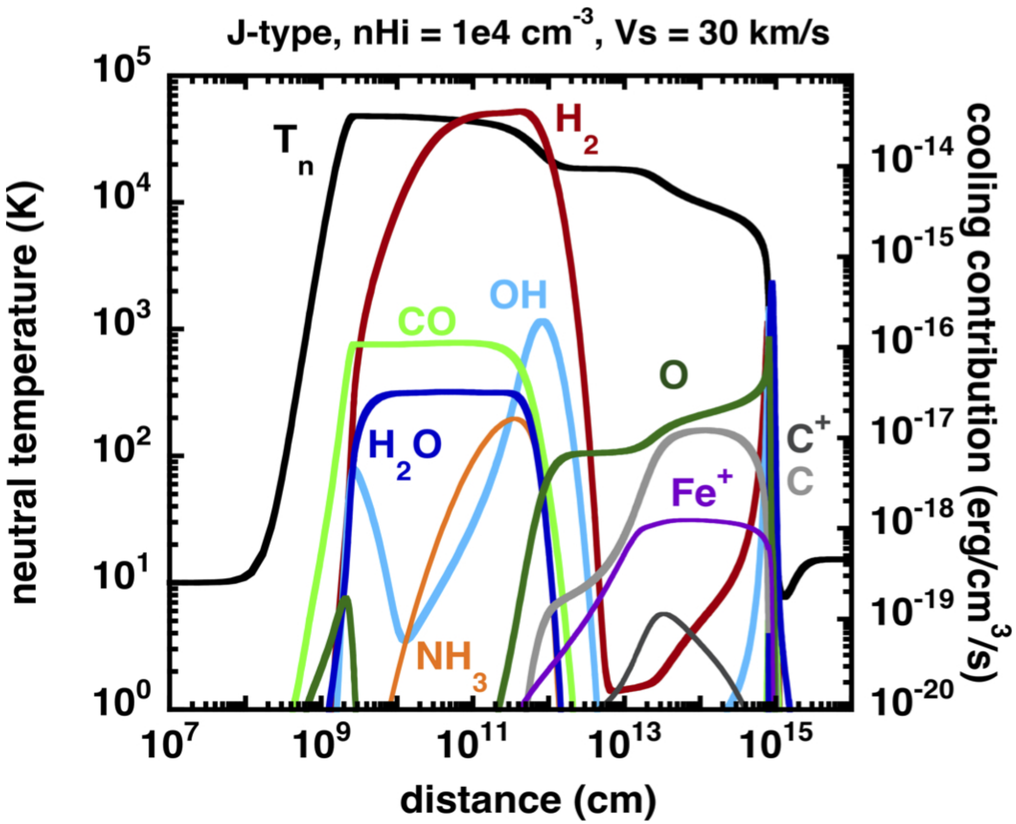

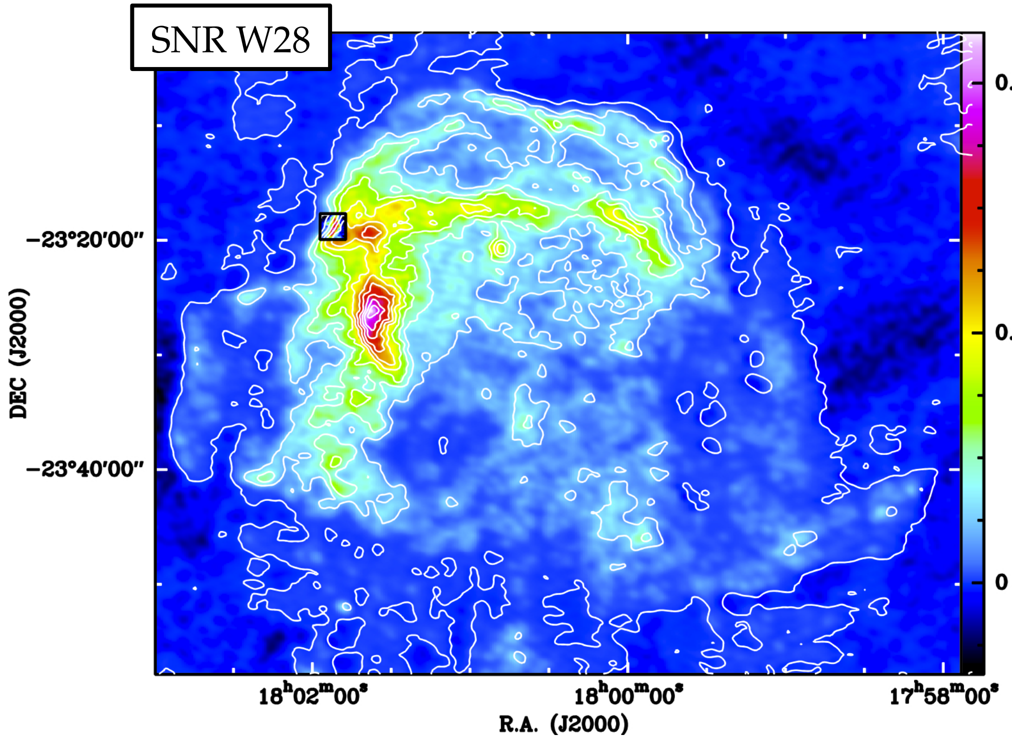

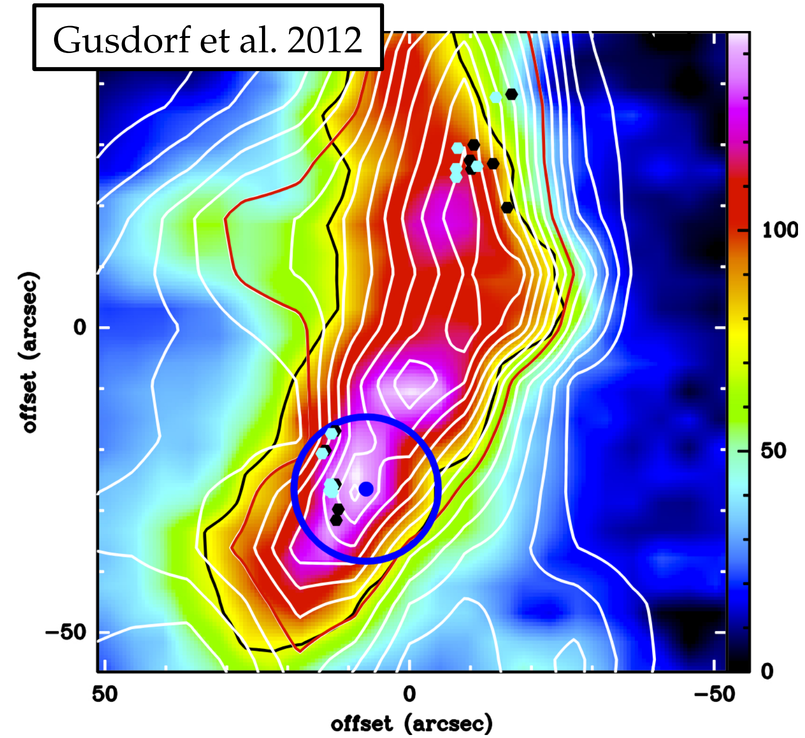

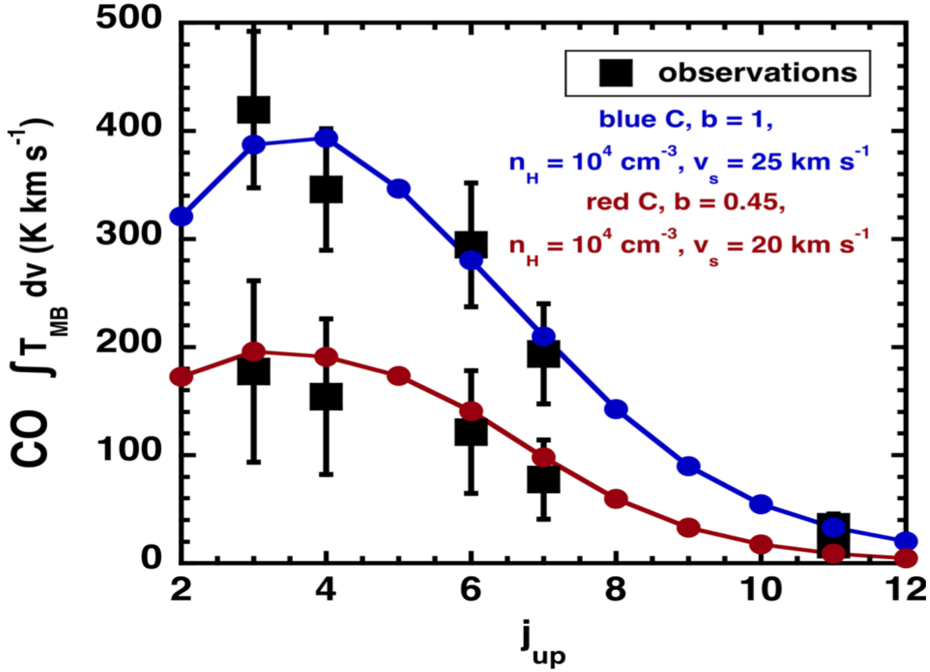

APEX, SOFIA observations

Analysis [level 3 / 3] : B. Meudon PDR code

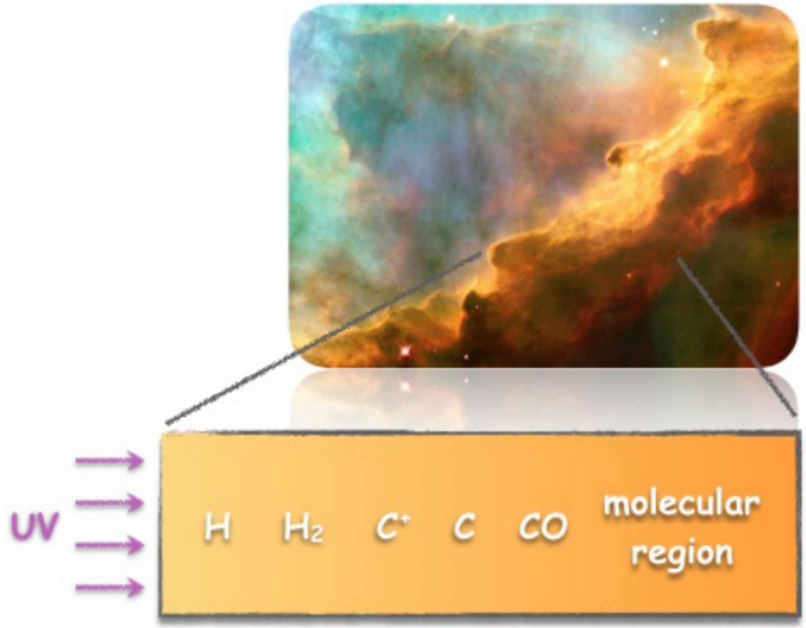

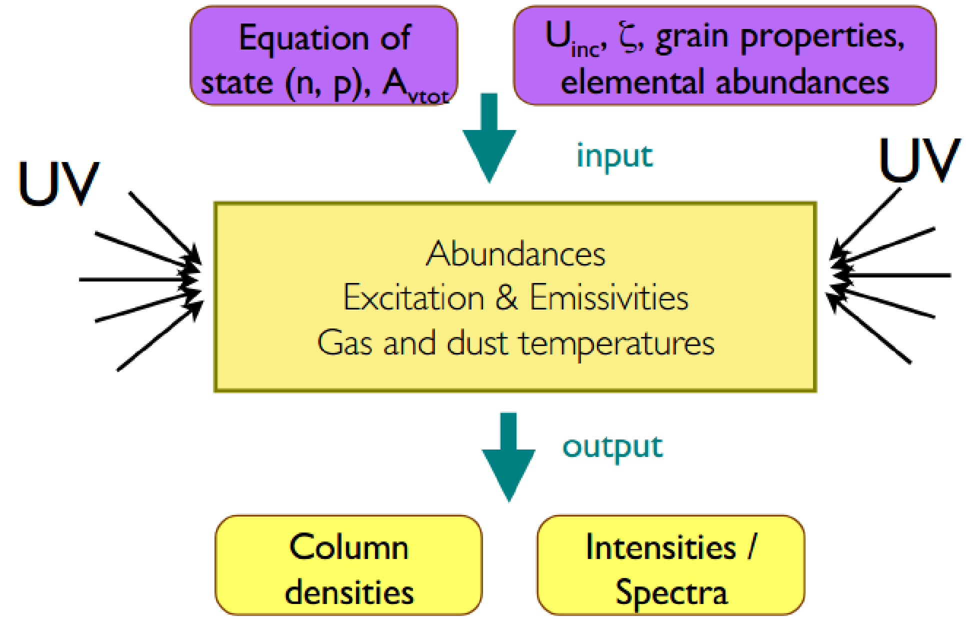

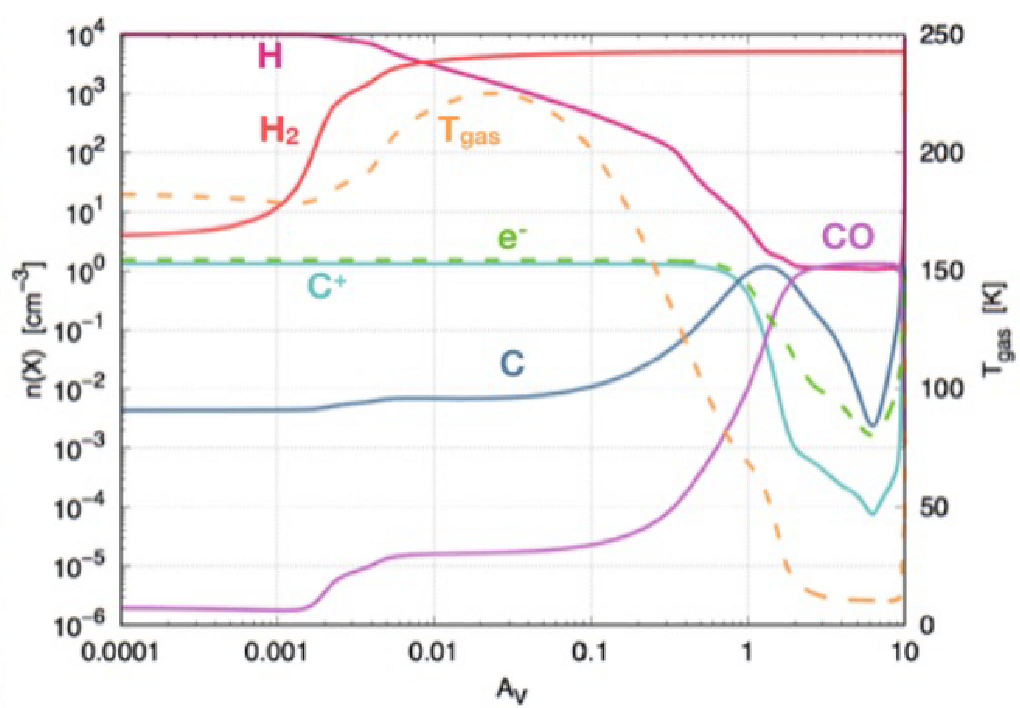

Dust phase
continuum observations

DUST PHASE : Continuum flux measurements

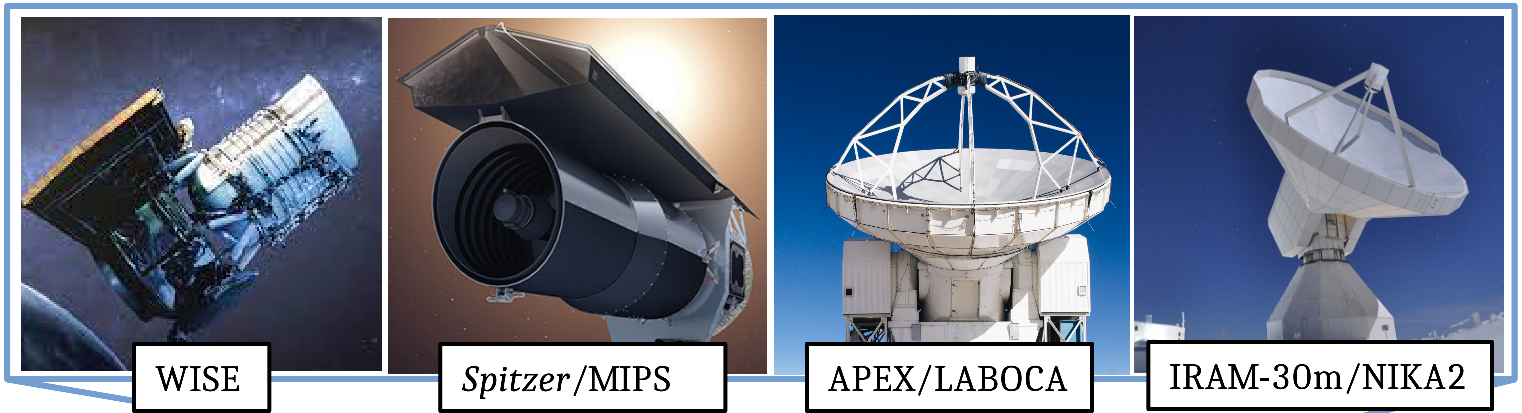

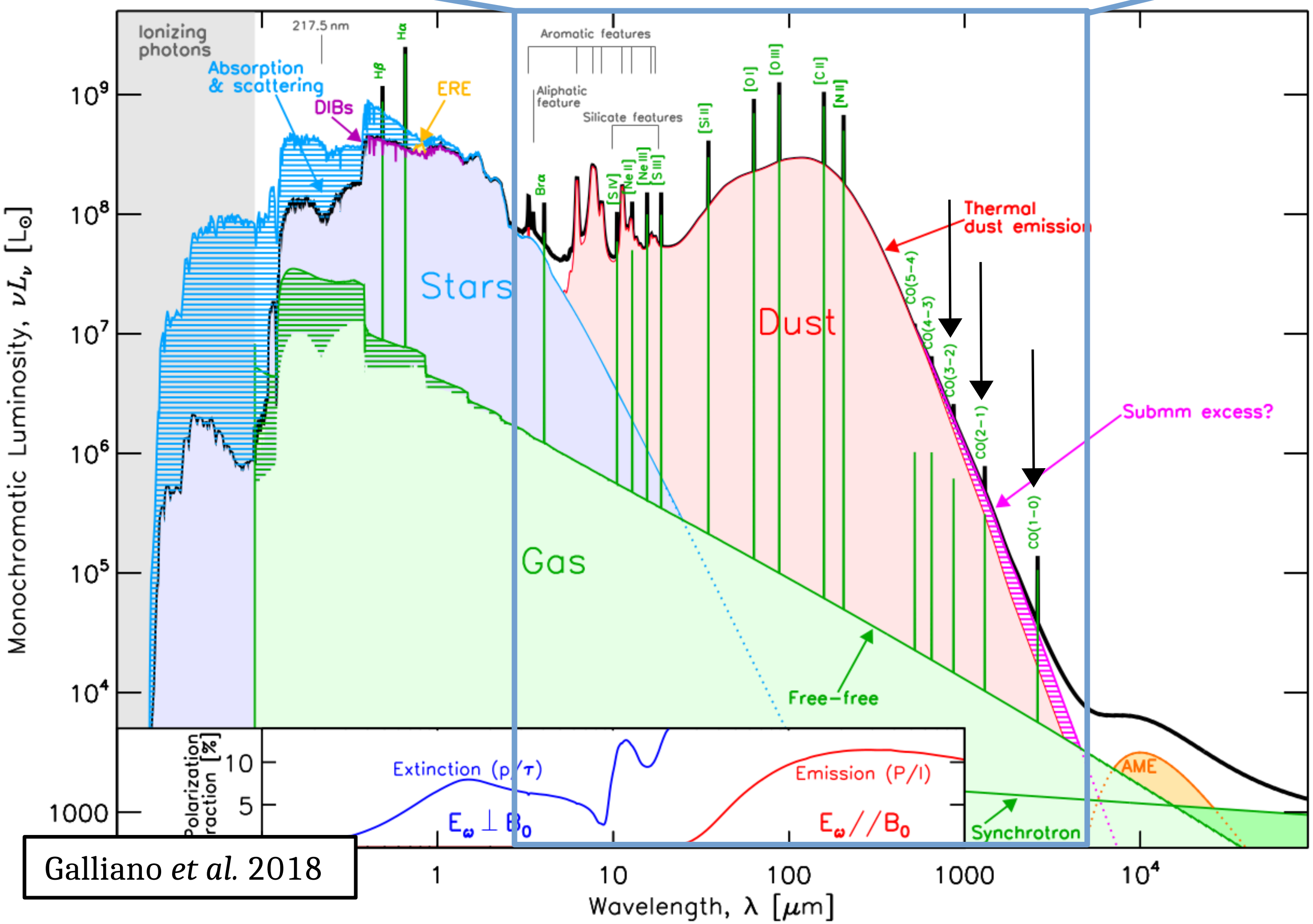

Galliano *et al.* 2018

Dust grains are heated by starlight, and cool by radiating in the infrared.

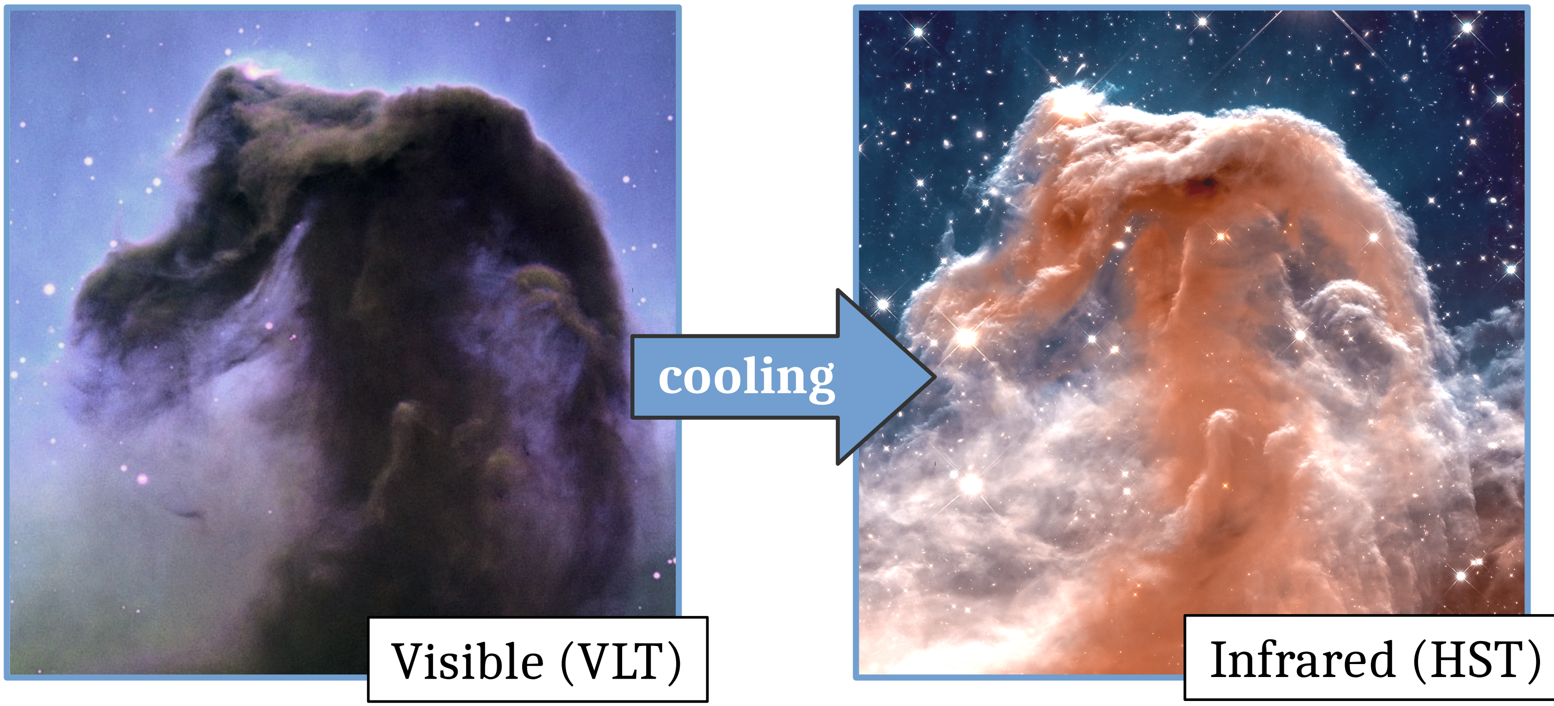

$$\left(\frac{dE}{dt}\right)_{\text{abs.}} = 4\pi a^2 \langle Q_{\text{abs}} \rangle u_\star c$$

$$\left(\frac{dE}{dt}\right)_{\text{emiss.}} = 4\pi a^2 \langle Q_{\text{abs}} \rangle \int B_\nu(T_{\text{d}}) d\nu$$

Dust grains are heated by starlight, and cool by radiating in the infrared.

Visible (VLT)

cooling

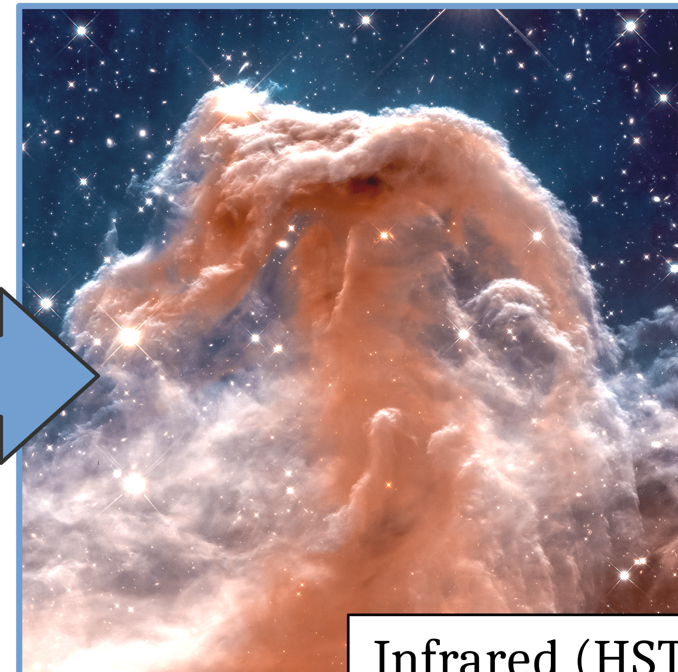

Infrared (HST)

$$\left(\frac{dE}{dt}\right)_{\rm abs.} = 4\pi a^2 \langle Q_{\rm abs} \rangle u_\star c$$

$$\left(\frac{dE}{dt}\right)_{\rm emiss.} = 4\pi a^2 \langle Q_{\rm abs} \rangle \int B_\nu(T_{\rm d}) d\nu$$

Steady state

$$\underbrace{L_\nu(\lambda)}_{\text{dust monochromatic luminosity}} = \underbrace{M_{\rm dust}}_{\text{dust mass}} \times \overbrace{\underbrace{\kappa(\lambda_0).\,(\lambda_0/\lambda)^\beta}_{\text{parametric opacity}} \times \underbrace{4\pi B_\nu(\lambda, T_{\rm dust})}_{\text{black body}}}^{\text{Modified Black Body (MBB)}}$$

The **PPMAP** procedure summarized in one equation (**Marsh et al. 2015**):

Column density (dust + gas)

Opacity index

$$I_\lambda = \sum_{k=1}^{N} \sum_{l=1}^{M} \left\{ \left(\frac{N(T_{\mathrm{d},k}, \beta_l)}{2.1 \times 10^{24}\ \mathrm{cm}^{-2}} \right) \left(\frac{\lambda}{300\ \mu\mathrm{m}} \right)^{-\beta_l} B_\lambda(T_{\mathrm{d},k}) \right\}$$

Dust optical depth

Modified Blackbody (MBB)

Sum on temperatures

Sum on opacity indices

The **PPMAP** procedure summarized in one equation (**Marsh et al. 2015**):

Column density (dust + gas)

Opacity index

$$I_\lambda = \sum_{k=1}^{N}\sum_{l=1}^{M}\left\{\left(\frac{N(T_{\mathrm{d},k},\beta_l)}{2.1\times10^{24}\ \mathrm{cm}^{-2}}\right)\left(\frac{\lambda}{300\ \mu\mathrm{m}}\right)^{-\beta_l} B_\lambda(T_{\mathrm{d},k})\right\}$$

Dust optical depth

Modified Blackbody (MBB)

Sum on temperatures

Sum on opacity indices

Dust thermal SED

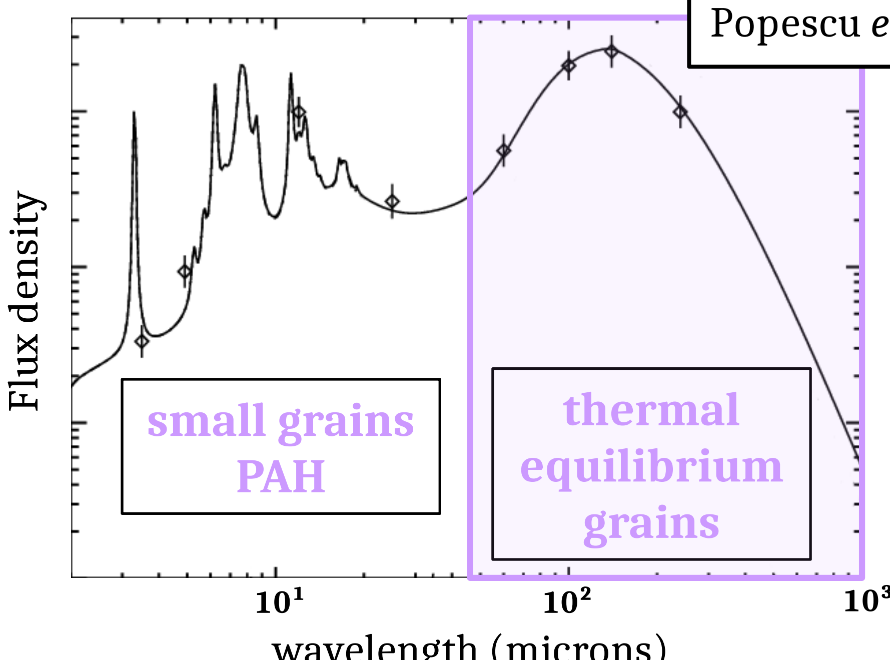

Popescu *et al.* 2010

→ Fair approximation for **thermal equilibrium grains**

→ Not for **very small grains** and **polycyclic aromatic hydrocarbons features (PAH)**

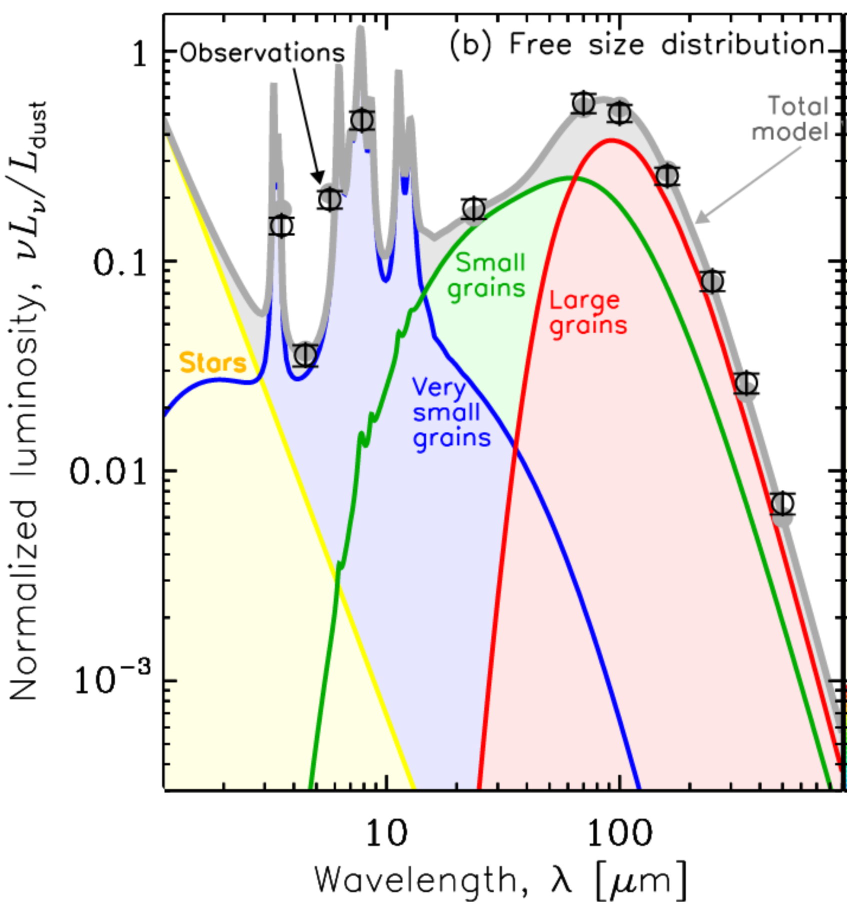

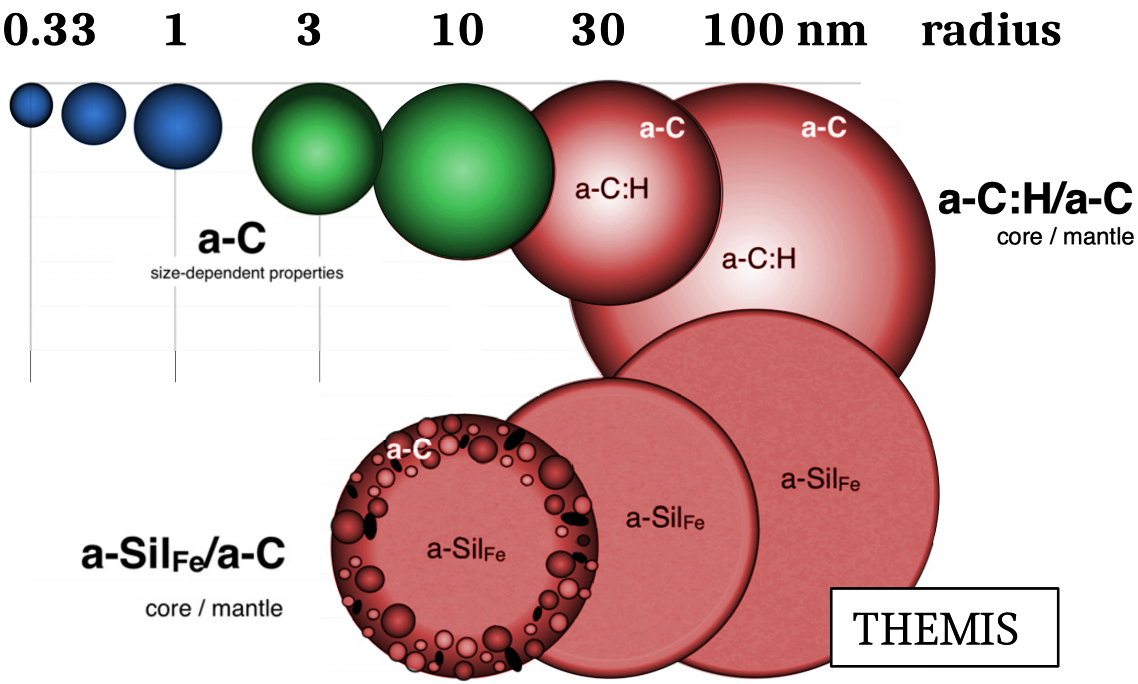

THEMIS

Jones *et al.* 2017

« **HiER**archical **B**ayesian **I**nference for dust **E**mission »

Galliano *et al.* 2018

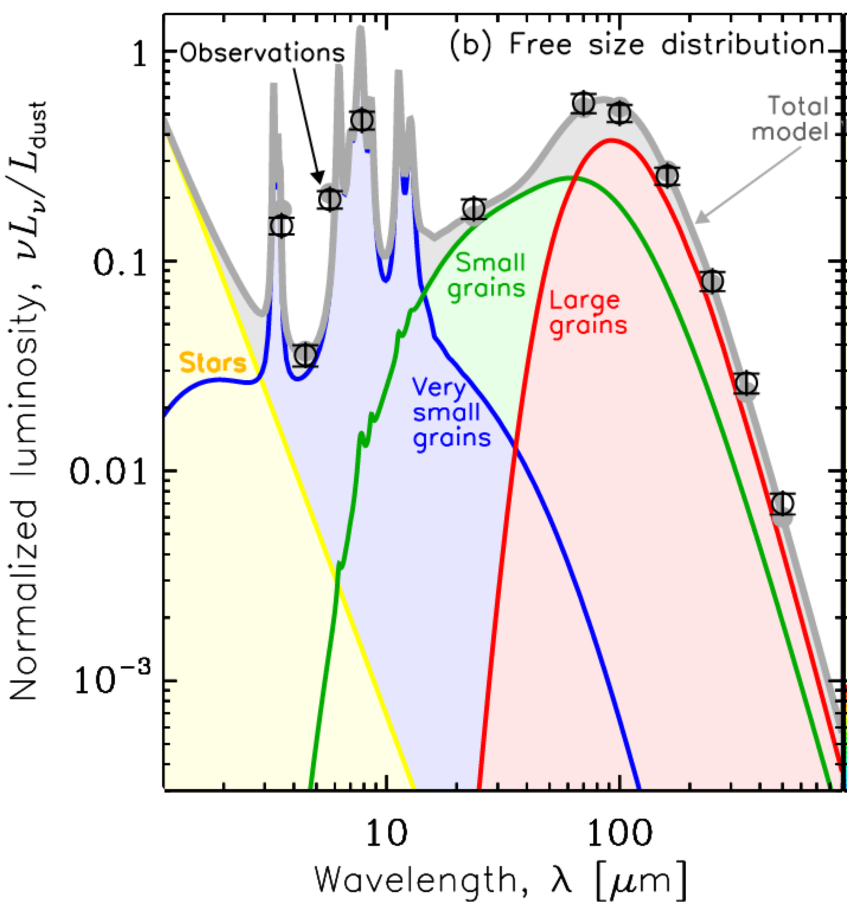

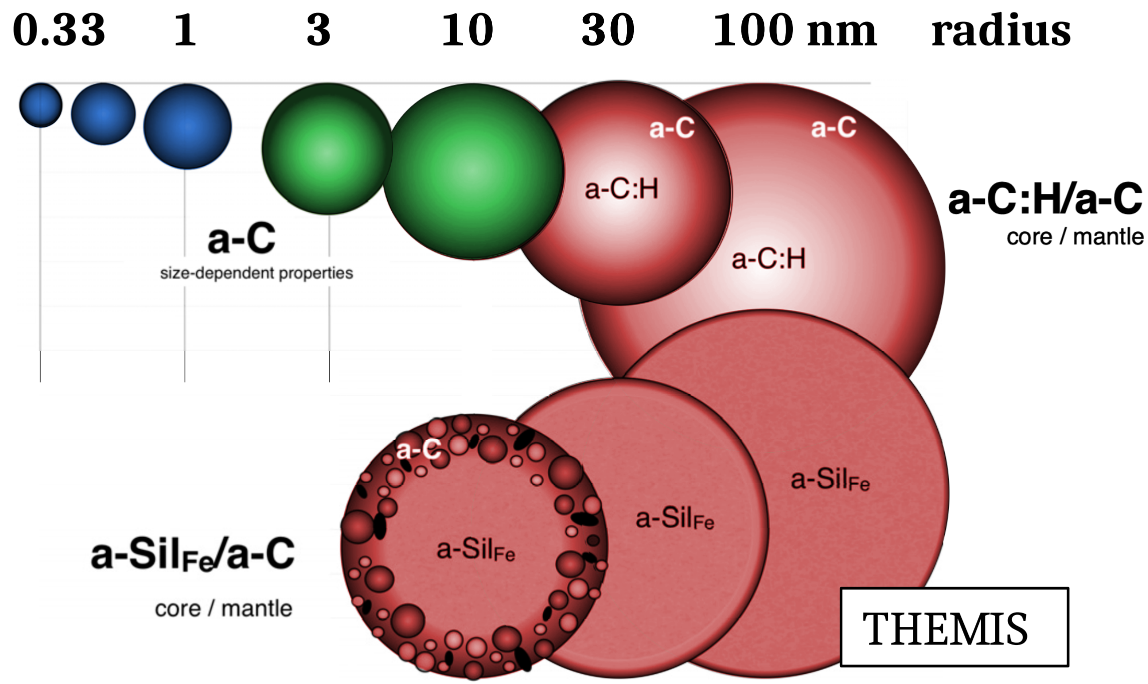

Jones *et al.* 2017

« **HiER**archical **B**ayesian **I**nference for dust **E**mission »

Galliano *et al.* 2018

HerBIE/THEMIS parameters

$$M_{\rm dust}$$ **mass**

$$U_{\rm min} \quad U_{\rm max} \quad \alpha$$ **ISRF**

$$q^{\rm PAH} \quad f^{\rm PAH^+}$$

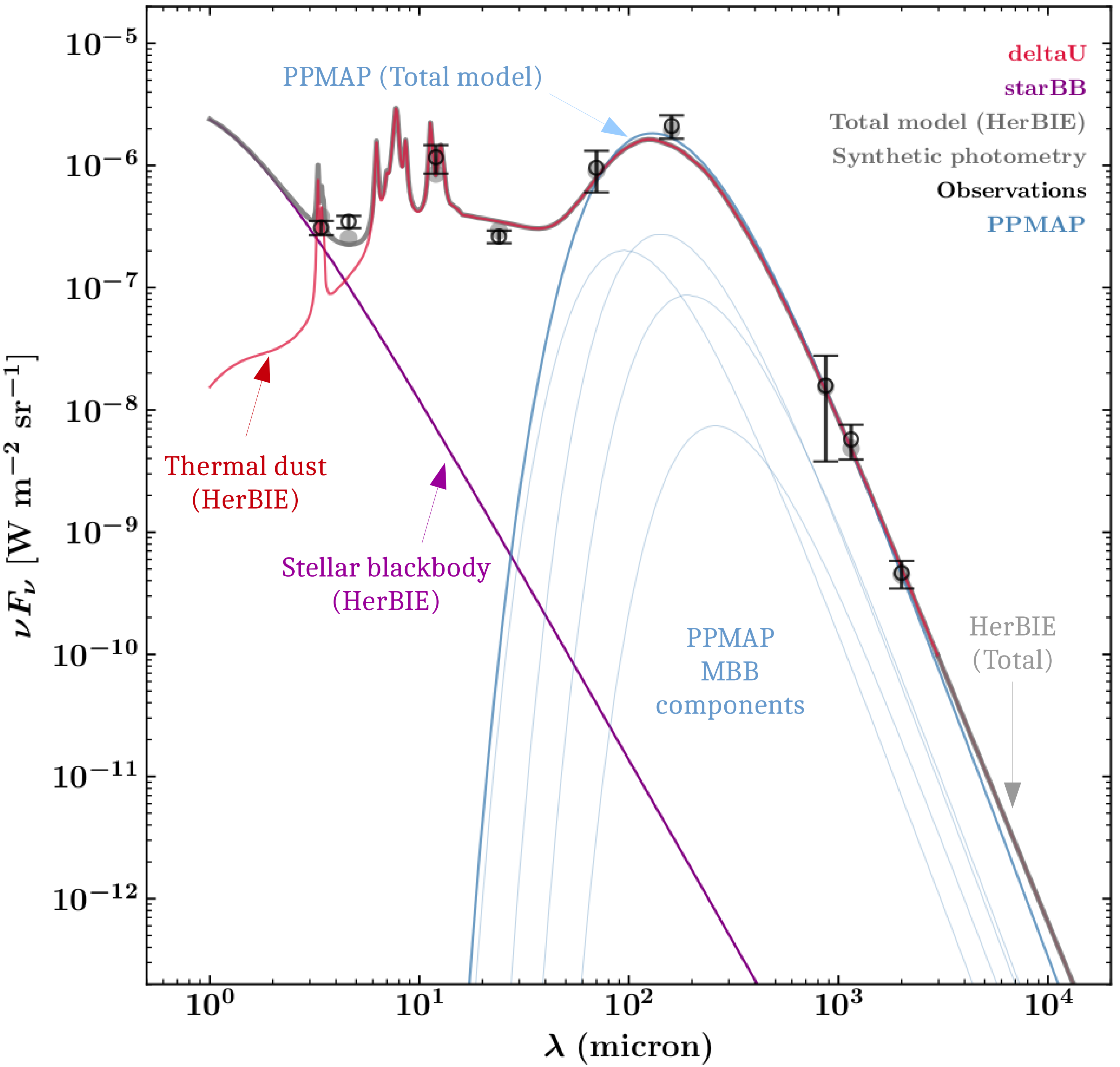

HerBIE :

$\chi^2 = 1.2$

PPMAP :

$\chi^2 = 1.5$

Opacity index :

$\beta \sim 1.8$

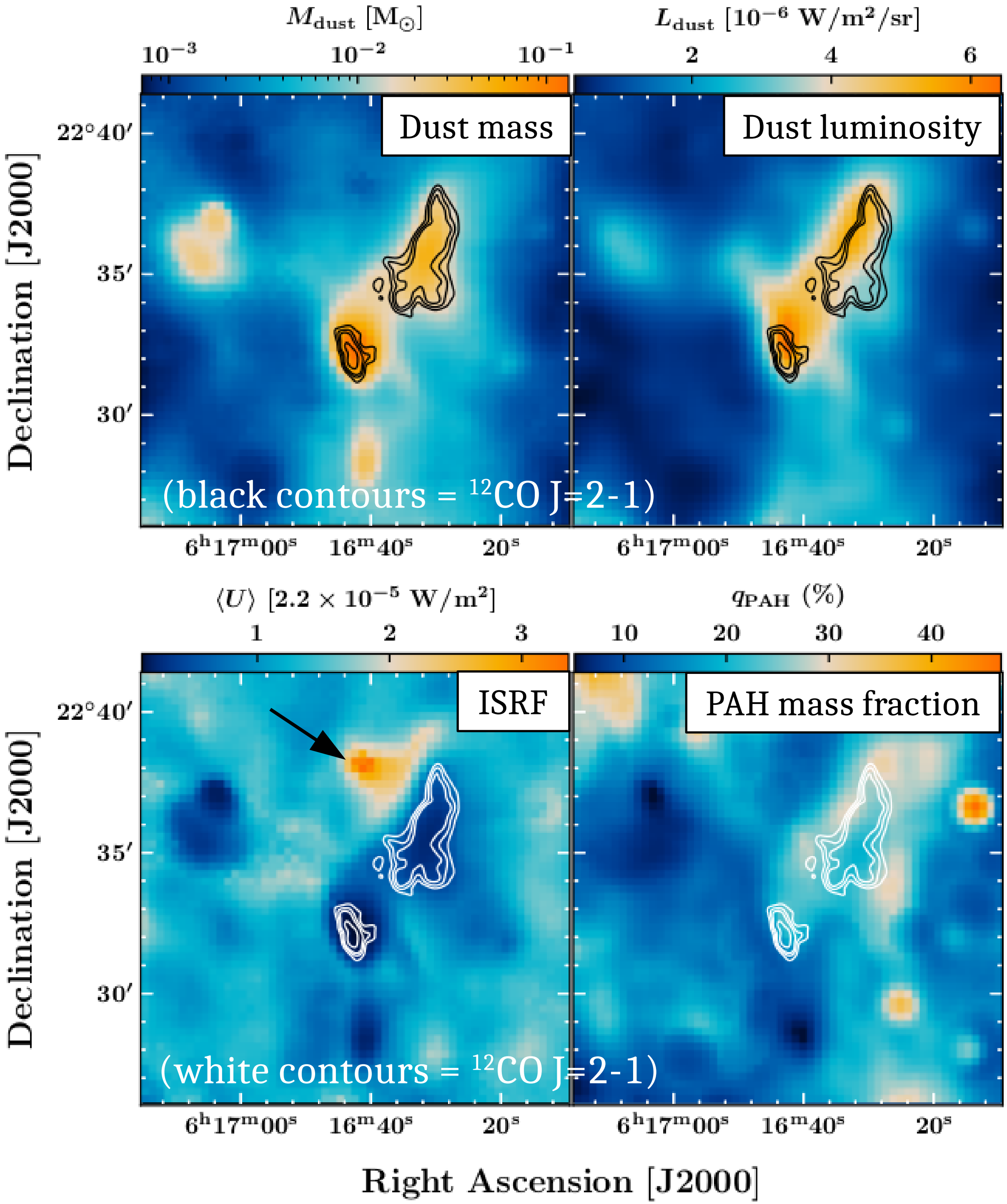

HerBIE :

- Total dust mass

- Total dust luminosity

- Interstellar radiation field intensity (diffuse Galactic ISM : U=1)

$$\int_{0.0912\ \mu m}^{8\ \mu m} 4\pi J_\lambda d\lambda = 2.2\times10^{-5}\ W/m^2$$

- PAH mass fraction

Magnetic field

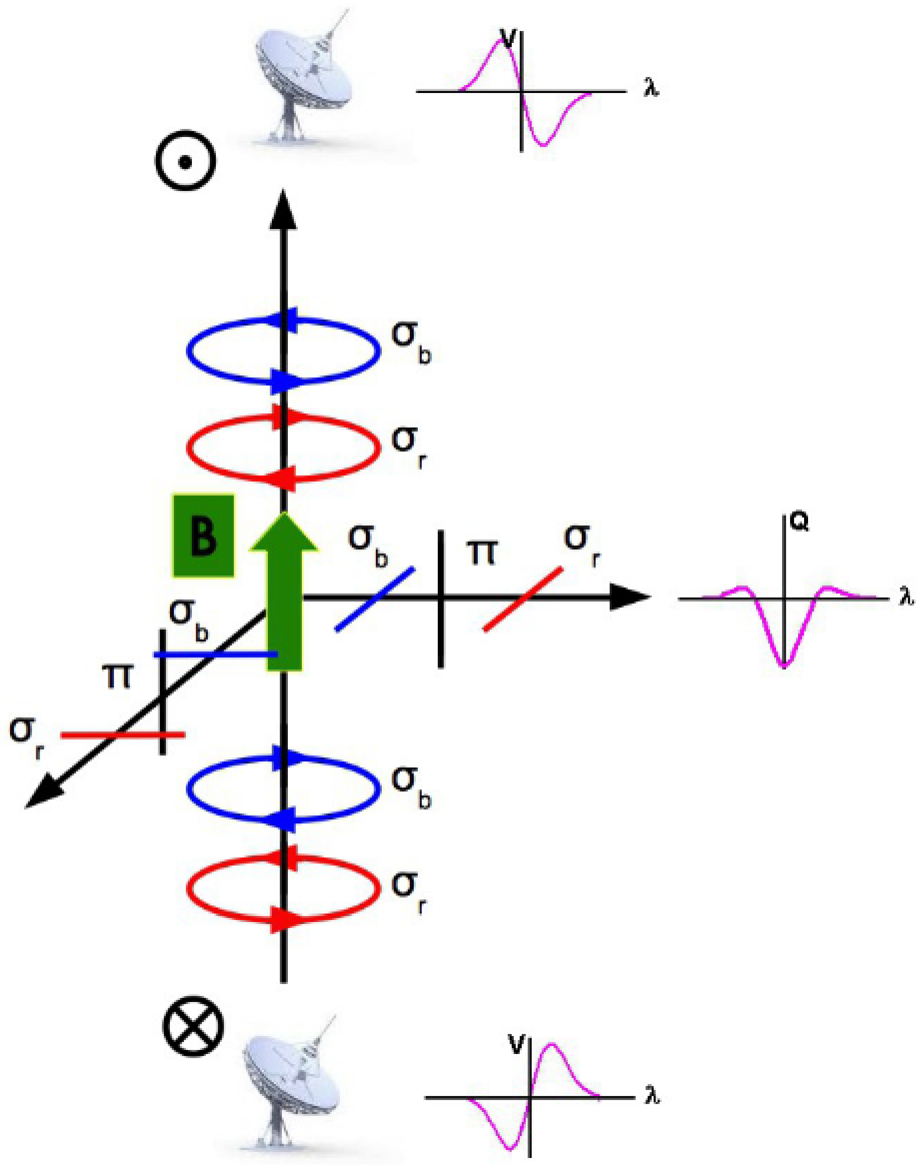

Zeeman effect on Molecular lines

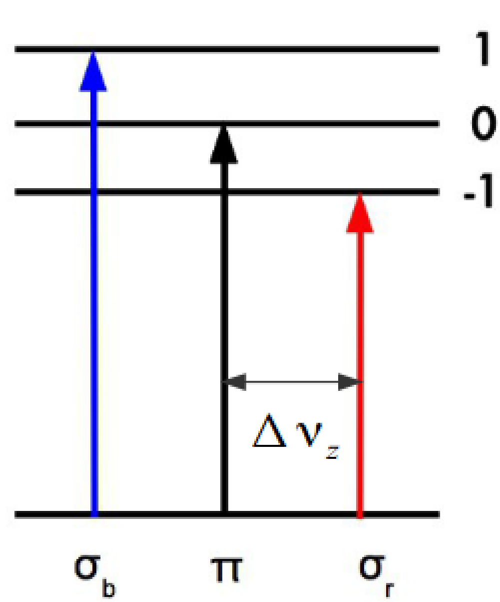

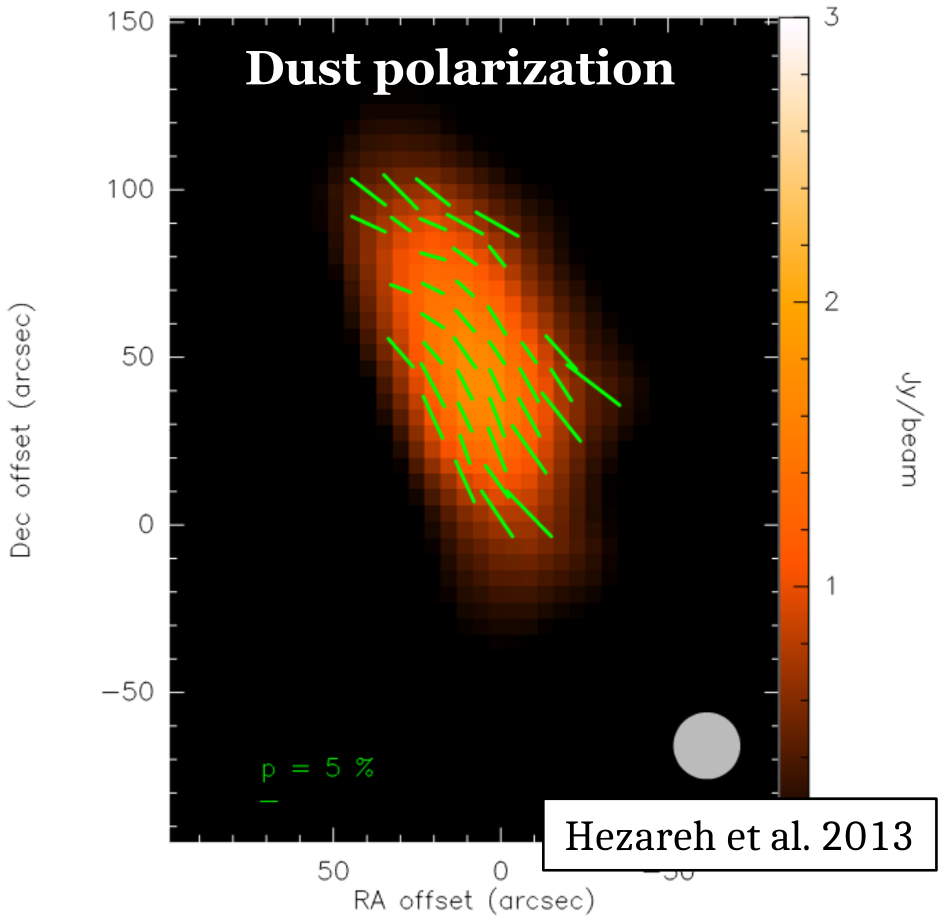

Hezareh et al. 2013

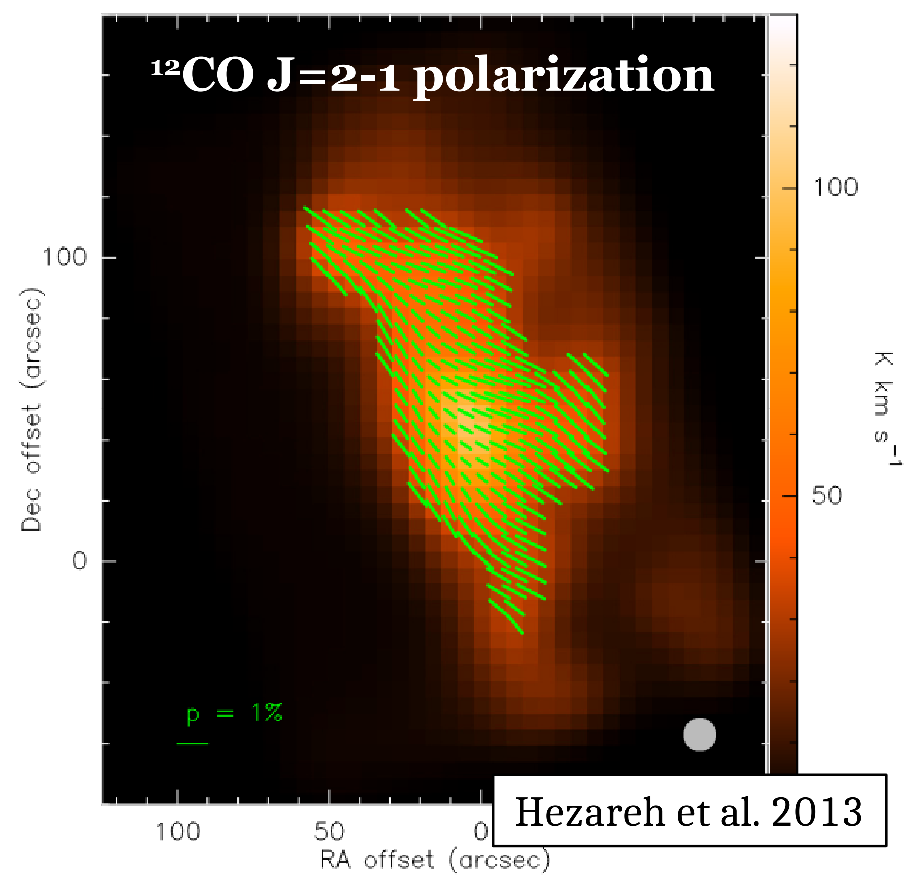

Hezareh et al. 2013

See also Houde et al. 2012

Protostars

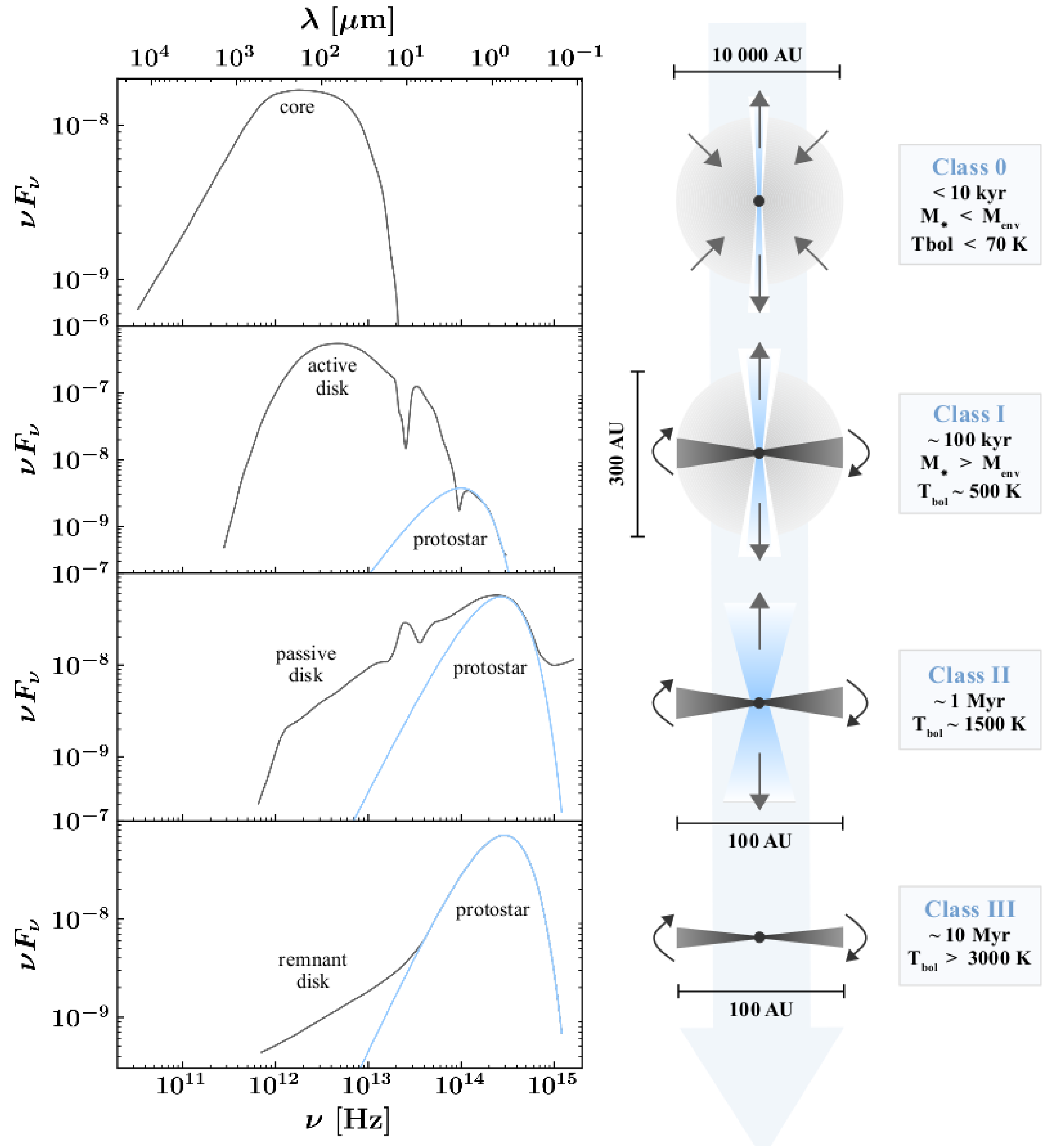
λ [μm]
10^4 10^3 10^2 10^1 10^0 10^{-1}
νF_ν
core
active
disk
protostar
passive
disk
protostar
remnant
disk
protostar
10^{11} 10^{12} 10^{13} 10^{14} 10^{15}
ν [Hz]
10 000 AU
300 AU
100 AU
100 AU
Class 0
< 10 kyr
$M_* < M_{env}$
Tbol < 70 K
Class I
~ 100 kyr
$M_* > M_{env}$
T_{bol} ~ 500 K
Class II
~ 1 Myr
T_{bol} ~ 1500 K
Class III
~ 10 Myr
T_{bol} > 3000 K

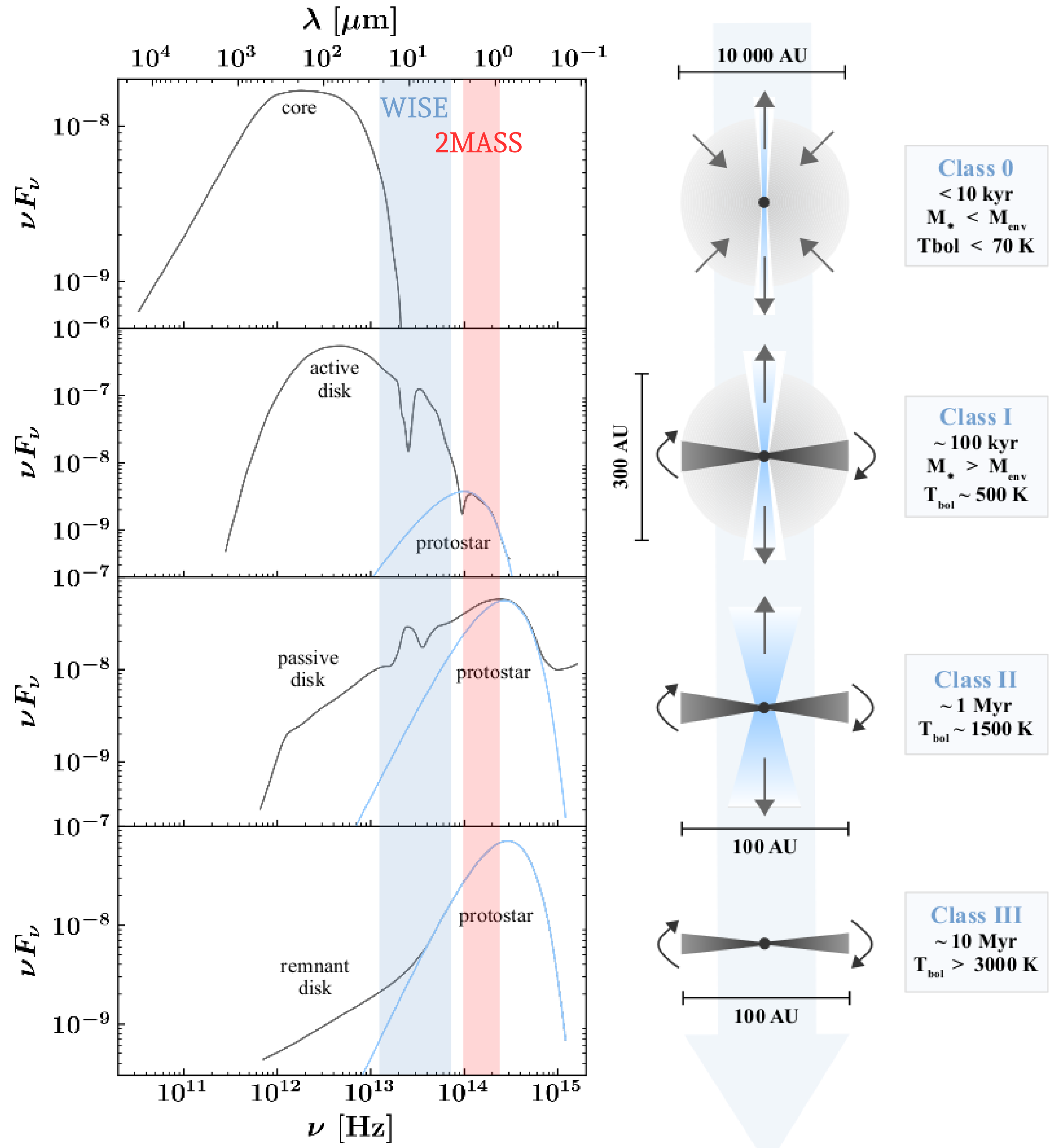
λ [μm]
10^4 10^3 10^2 10^1 10^0 10^-1
core
WISE
2MASS
active disk
protostar
passive disk
protostar
remnant disk
protostar
νF_ν
10^11 10^12 10^13 10^14 10^15
ν [Hz]
10 000 AU
300 AU
100 AU
100 AU
Class 0
< 10 kyr
M* < Menv
Tbol < 70 K
Class I
~ 100 kyr
M* > Menv
Tbol ~ 500 K
Class II
~ 1 Myr
Tbol ~ 1500 K
Class III
~ 10 Myr
Tbol > 3000 K

WISE census

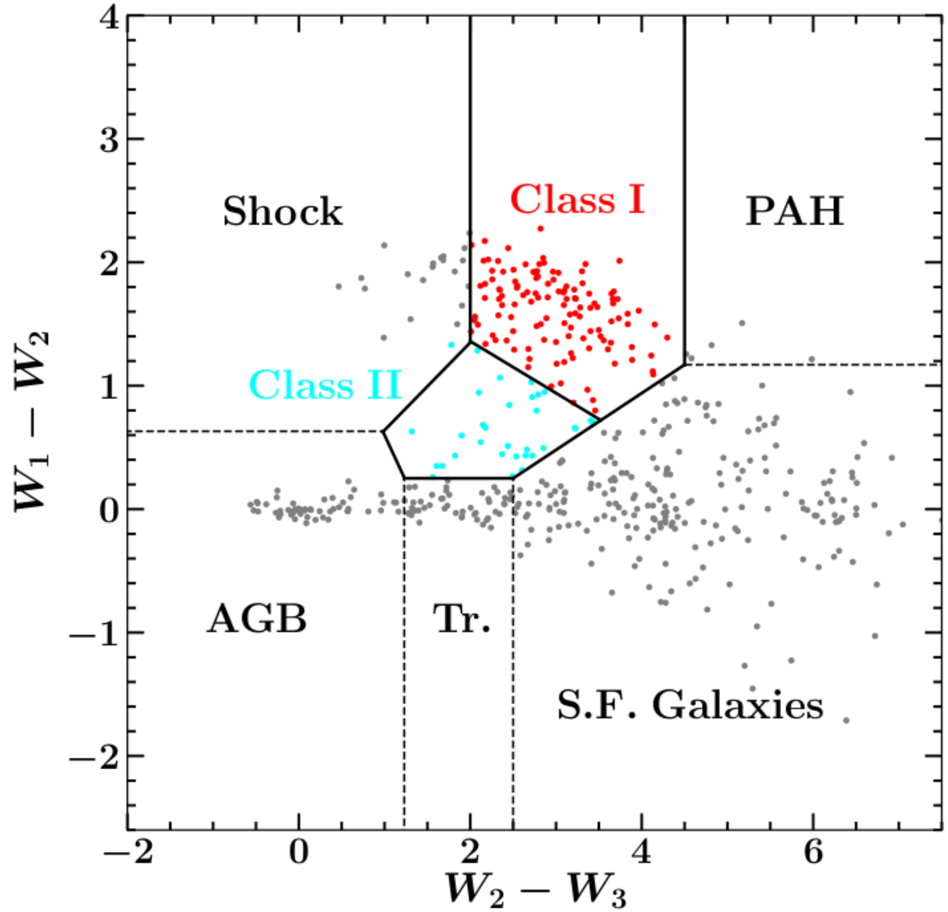

Fischer *et al.* 2016

2MASS census

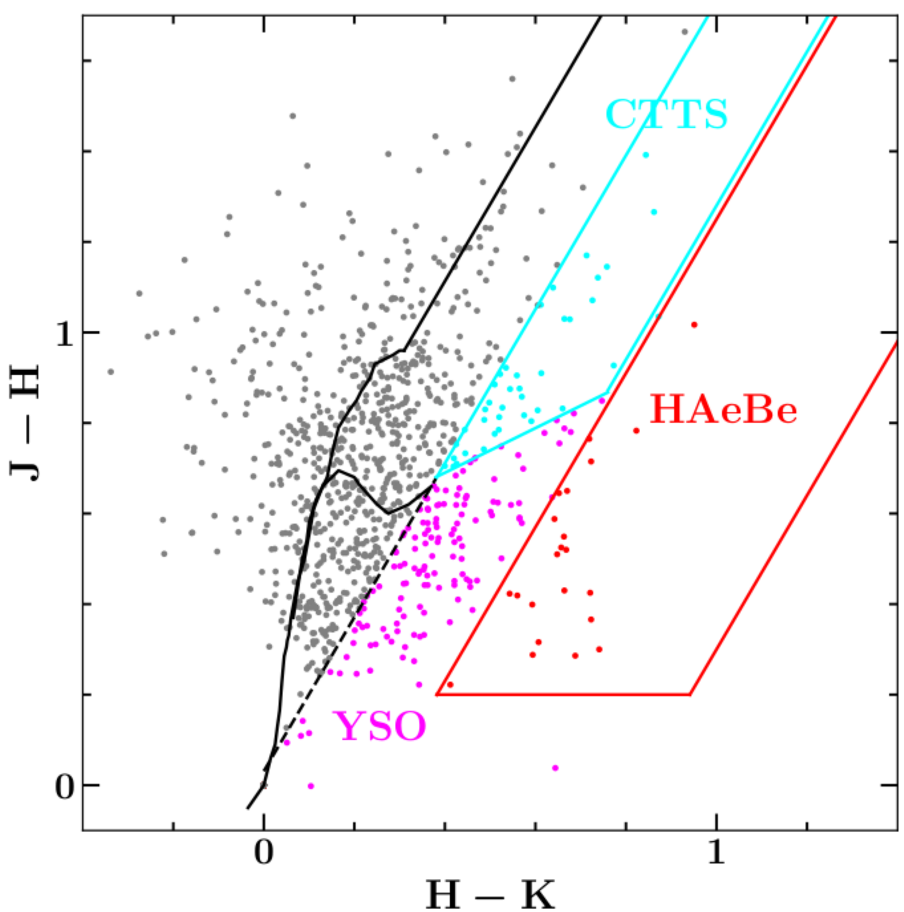

Xu *et al.* 2011

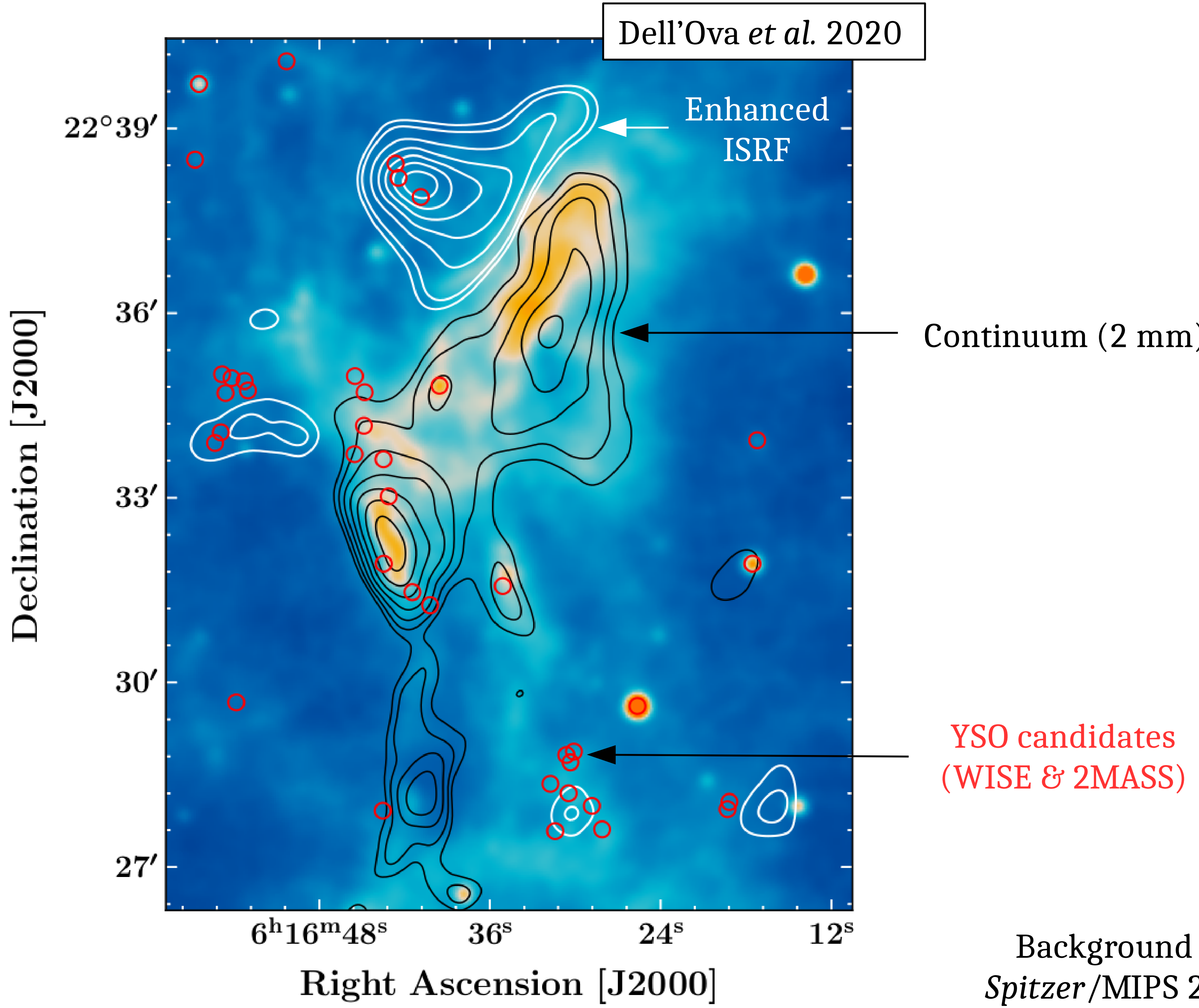

Background image :
Spitzer/MIPS 24 micron

Summary

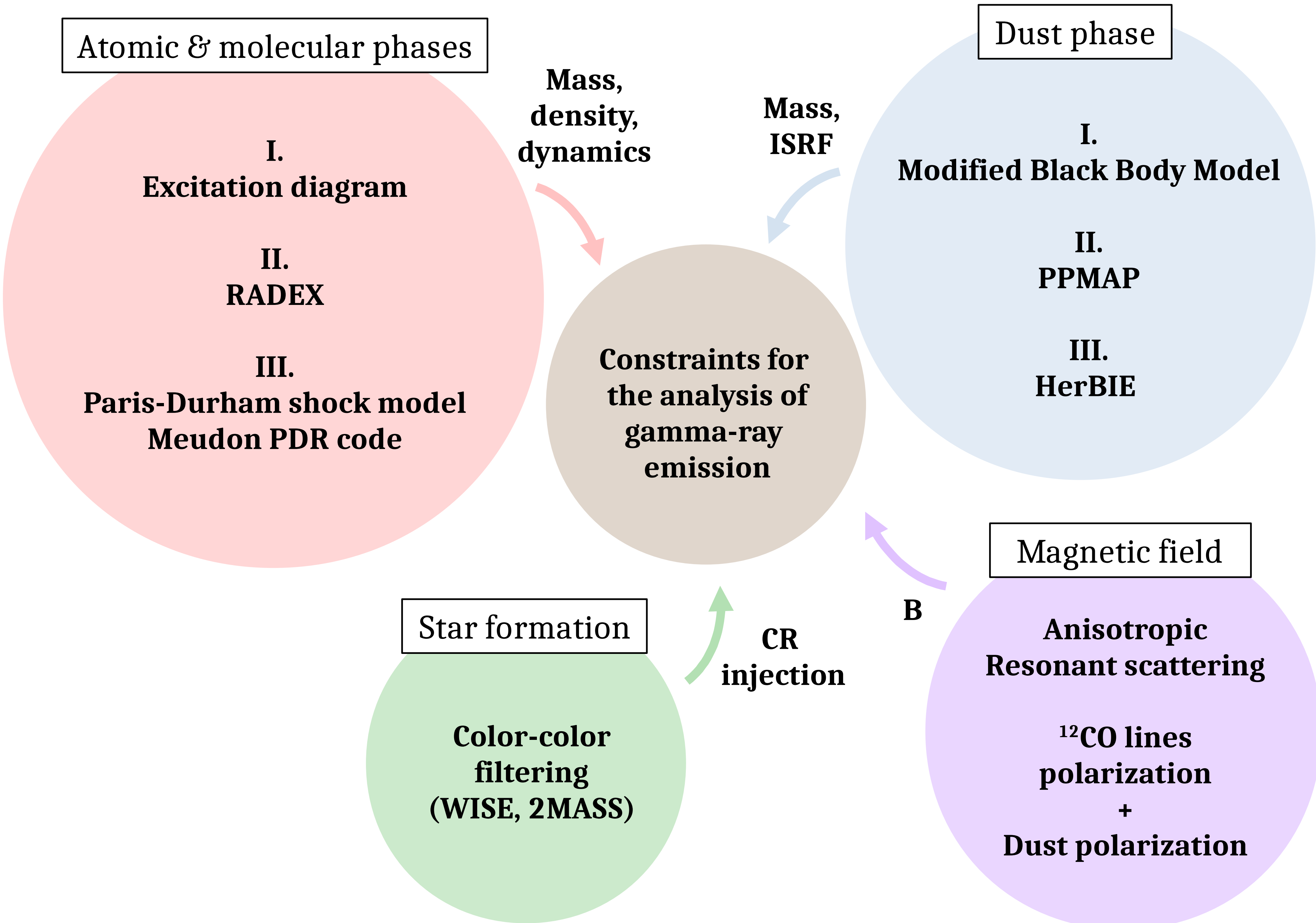
Atomic & molecular phases
I.
Excitation diagram
II.
RADEX
III.
Paris-Durham shock model
Meudon PDR code
Mass, density, dynamics
Mass, ISRF
Dust phase
I.
Modified Black Body Model
II.
PPMAP
III.
HerBIE
Constraints for the analysis of gamma-ray emission
Star formation
Color-color filtering
(WISE, 2MASS)
CR injection
B
Magnetic field
Anisotropic Resonant scattering
12CO lines polarization
+
Dust polarization